UNIVERSITY OF CALIFORNIA,
IRVINE

Instability of the Two-Stream Electron-Beam System

DISSERTATION

submitted in partial satisfaction of the requirements
for the degree of

DOCTOR OF PHILOSOPHY

in Mathematics

by

Katherine Evans

Dissertation Committee:
Professor Alexander Figotin, Chair
Professor Svetlana Jitomirskaya
Professor Abel Klein

2019

TABLE OF CONTENTS

ACKNOWLEDGMENTS

I would like to thank my advisor, Professor Alex Figotin, for his guidance and time. I would also like to thank my family and Nishant for their continued support and infinite patience.

CURRICULUM VITAE

Katherine Evans

EDUCATION

Doctor of Philosophy in Mathematics **2019**
University of California, Irvine *Irvine, California*

Master of Science in Mathematics **2015**
University of California, Irvine *Irvine, California*

Bachelor of Arts in Mathematics **2013**
University of California, Irvine *Irvine, California*

RESEARCH EXPERIENCE

Graduate Research Assistant **2013–2019**
University of California, Irvine *Irvine, California*

TEACHING EXPERIENCE

Teaching Assistant **2013–2019**
University of California, Irvine *Irvine, California*

ABSTRACT OF THE DISSERTATION

Instability of the Two-Stream Electron-Beam System

By

Katherine Evans

Doctor of Philosophy in Mathematics

University of California, Irvine, 2019

Professor Alexander Figotin, Chair

The physical phenomenon of amplification in traveling wave tubes can be understood mathematically as a result of system instability or exponentially growing eigenmodes. We study here instability in the uncoupled multi-stream electron beam model, focusing primarily on properties and solutions of the characteristic equation associated with the beam. In particular, we show that in general the zeroes of the characteristic function are distinct. Then, in the two-stream case, we construct a series representation of frequency-dependent solutions to the electron beam characteristic equation near the frequency at which these solutions transition from non-real (unstable eigenmodes) to real (oscillatory eigenmodes).

List of Symbols and Acronyms

$\bar{\beta}$	electron beam parameter
$\bar{\gamma}$	TWT-system parameter
$\bar{\theta}$	MTL integral parameter
$\bar{q}$	slow-wave structure
$\beta_s = \frac{\sigma_B}{4\pi}\omega_{ps}^2$	electron beam parameter associated with s-stream
$\breve{\omega}$	dimensionless frequency
$\Delta_B(u)$	e-beam function
$\Delta_T(u)$	MTL function
$E(t,z) = \sum_s E_s(t,z)$	total axial electric field
$(a,b) = a * B = \sum a_s * a_b$	scalar product of vectors a and b with complex valued entries a_s and b_s, respectively
$\mathbf{E}$	electric field
$\mathbf{J}$	current
$\mathring{n_s}$	electron constant density for a stationary state, time and space independent constant density
$\mathring{v}_s$	electron constant velocity for a stationary state, time and space independent constant
$\mathscr{D}(u,\bar{\gamma})$	TWT-system characteristic function

$\mathscr{D}_B(u)$	normalized characteristic function of the e-beam
$\mathscr{D}_T(u)$	normalized characteristic function of the MTL
$D_B(u)$	characteristic functions of the electron beam
$D_T(u)$	characteristic functions of the MTL
ω	frequency which is assumed to be real in most of the cases
$\omega \to \Re(k(\omega))$	dispersion relation for an unstable modal branch
ω_{ps}	plasma frequency of s-stream
${\omega_{ps}}^2 = \frac{4\pi \mathring{n_s} e^2}{m}$	the square of the electron plasma frequency associated with density $\mathring{n_s}$
ω_w	pulse (wave-packet) shifted frequency
$\Re(\zeta), \Im(\zeta)$	respectively the real and the imaginary parts of a complex number ζ
σ	conductivity
σ_B	the area of the cross-section which is the same for every electron s-stream
θ_s	MTL parameters
ζ^*	complex conjugate to a complex number ζ
A^*	adjoint (Hermitian adjoint) to a matrix A, that is $(a, Ab) = a^*Ab = (A^*a, b)$ and $[A^*]_{ij} = {A^*}_{ji}$ (for a non-square matrix A the scalar products $(\cdot, \cdot)$ are associated with relevant (different) spaces)
a^*	Hermitian conjugate to a vector a, that is if a is a column vector then a^* is row vector with components $[a^*]_s = {a^*}_s$
a^T	vector transposed to vector a, that is if a is a column vector then a^T is row vector; $a^T = a^*$ for a with real entries

A^T	matrix transposed to matrix A
b	coupling (between the MTL and the electron beam) vector
C	MTL matrix of mutual capacitance that can be position dependent, that is $C = C(z)$
$E_s(t, z)$	axial generated electric field for s-stream
h_ω	space-charge function
$I(z, t) = \{I_j(z, t)\}$	currents associated with MTL
k	wave number which can be a complex number
$K(u) = \frac{\Omega(u)}{u}$	TWT-system wavenumber function (complex-valued)
$k\omega$-node	instability node of the dispersion-instability graph
L	MTL matrix of mutual inductance that can be position dependent, that is $L = L(z)$
m	electron mass
n_B	number of electron streams in the electron beam
n_T	number of transmission lines in the MTL
n_s	charge wave density
$N_s(t, z)$	electron volume density for s-stream
$Q(z, t) = \{Q_j(z, t)\}$	charges associated with MTL
$q(z, t) = \{q_s(z, t)\}$	charges associated with electron streams
$u = \frac{\omega}{k}$	phase velocity which can be a complex number
u_{en}	energy phase velocity
u_{gr}	wave-packet group velocity
u_w	wave-packet (pulse) phase propagation velocity
$V(z, t) = \{V_j(z, t)\}$	voltages associated with MTL
$v = O(u)$	the absolute value of ratio v/u of quantities v, v is bounded by a finite positive constant

$v = o(u)$	quantities v and u satisfy $\lim v/u = 0$
$\mathring{v}_s$	charge wave velocity
$\mathring{v}_s(t, z)$	axial velocity for s-stream
w_s	MTL characteristic velocities
z	axis of TWT
e-beam	electron beam
MSB system	multi-stream e-beam system
msb-system	multi-sream e-beam system of equations
MTL	multi-transmission line
RF	radio frequency
SWS	slow-wave structure
TL	transmission line
TWT	traveling wave tube
TWT-system	multi-stream electron beam coupled to the MTL

Chapter 1

Introduction

1.1 Overview

Our main goal is to understand amplification due to system instability in *traveling wave tubes* (TWTs), vacuum electronic devices consisting of an electron beam interacting with a *slow-wave structure* (SWS) used to amplify radio-frequency (RF) signals. The TWT's ability to amplify radio-waves across long distances, to reach high signal amplitude with low noise, and to handle large bandwidth high-frequency signals makes it an ideal system for data transmission in satellites and space probes. There is a long history of modeling these devices beginning as early as the 1930s and 1940s ([25], [7]); however, one of the simplest yet effective models of a TWT was given by J. R. Pierce in 1950. He constructed a one-dimensional, linear model of a TWT system that is still used for some design estimates today [22],[23].

Since the 1950s, many authors have extended and generalized Pierce's model to aid in design optimization as well as to better understand physical phenomena such as amplification and e-beam energy transfer. There are several nonlinear theories of TWT systems (see [26],

[14], and [29], for example) that treat beam-wave dynamics in detail, though they are quite complex and typically require heavy numerical analysis.

In 2013, A. Figotin and G. Reyes constructed the first Lagrangian field theory model of a TWT that generalized Pierce's theory to include possibly inhomogeneous MTL coupled with the beam which was modeled in the same vein as Pierce's electron beam [10]. This theory allowed the authors to study amplification and energy transfer and more complex slow-wave structures while keeping the simplicity and constructiveness presented in the Pierce model. As such, the MSB model of the TWT system studied in the remainder of this text begins with the original Pierce model and its generalization to an MTLB system by [10].

The idea to generalize representation of the e-beam to multiple streams of electrons has been studied by several authors including [8],[4], [3], and [28]. In 2018, A. Figotin further extended this theory to include multi-stream flows in the electron beam. This development allows the model to account for electron plasma phenomena such as electron debunching, two-beam instability, Landau damping, and more. Development of an analytic theory of the TWT-system studies the system Lagrangian, field equations, characteristic equation and eigenmodes of the multi-stream MTLB.

Our focus in this thesis is on the two-stream MSB system. Two-stream instability is a subject in plasma physics which has been studied extensively by various authors such as [6], [20], [2], [18], [19], [21], [24], [28].

A TWT consists of an electron beam interacting with a *slow-wave structure* (SWS), and as established by A. Figotin and G. Reyes in [10], the TWT can be modeled by the *multi-stream e-beam system* (MSB) in which we represent the e-beam by multiple streams of electrons (MSB) and the SWS by a multi-transmission line (MTL). Our primary topics of interest here are solutions to characteristic equations associated with the electron beam in the uncoupled system and their properties. We study system instability arising from non-

real, frequency-dependent solutions (phase velocities) to the characteristic equation of the MSB system. As these solutions can be real or non-real depending on the given frequency, the spectral theory of the MSB system is not commonly considered. However, making use of Lagrangian formulation of the MSB system, we are nonetheless able to study the transition from stable oscillatory solutions (corresponding to real eigenvalues) to unstable exponentially growing solutions (corresponding to non-real eigenvalues). In particular, we show that solutions near the transition point at which solutions become real or-nonreal, can be represented analytically by a Puiseux series. Moreover, we show that non-real solutions must have bounded imaginary part.

The structure of the text is as follows: in the remainder of Chapter 1 we briefly describe the operating principle of a TWT and it's applications, as well as the historical development of modeling an e-beam interacting with a wave-guide. In what follows, we analyze the zero set of the inverse characteristic function associated with the electron beam $\Delta_B(u)$ showing that beam parameters can always be chosen to make the zeros distinct (Chapter 3). In what remains, we focus our studies on the two-stream case ($n_B = 2$) and study analytic properties of the frequency-dependent solutions to the characteristic equation, $\mathscr{D}_B(u) = 1/\omega^2$. Restricting our attention to the two-stream case is motivated by the fact that a single-stream e-beam system has no exponentially growing instability until it is coupled to the MTL, in which case it develops a high frequency instability band. In contrast, a multi-stream e-beam (in particular, a two-stream e-beam) uncoupled system already has low frequency instability bands due to multiple electron streams of different stationary phase velocities. In Chapter 4, we construct a series representation for solutions near the instability transition node and show that the imaginary part of non-real solutions is always bounded. In Chapter 5, we consider the case when the two-streams merge.

1.2 Brief description of TWT's and their applications

TWT's are amplification devices consisting of an elongated vacuum tube containing an electron beam that passes through a radio frequency circuit (slow-wave structure). They are used in areas such as satellite communication, radar systems, and electronic warfare as electronic counter measure devices, i.e. to amplify decoy signals.

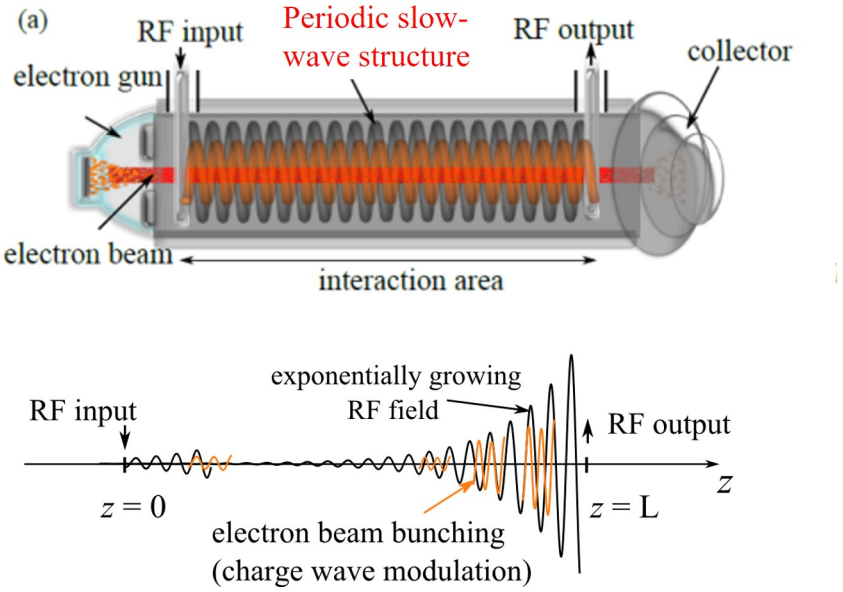

TWTs belong to a class of microwave devices (or *microwave tubes*) that amplify signals via Cherenkov radiation. As a result of interaction between the electron beam and a properly designed slow-wave-structure, the kinetic energy of the electrons is converted into electromagnetic energy stored in the field [15]. At one end of the TWT, a low-powered radio signal is fed into the RF cirucit. The signal travels along the tube at about the same speed as the electron beam, the electromagnetic (EM) field acts upon the beam and causes electron bunching, producing the space-charge wave. The EM field associated with the wave induces more current into the RF circuit and enhances the electron bunching. As the EM field builds up, it is amplified as it passes down the structure until a saturation regime is reached and a large RF signal is collected at the output.

1.3 Pierce's model of the TLB

In 1951, J.R. Pierce presented a linear, one-dimensional mode describing the interaction of an electron beam with a surrounding wave guide [22, 23]. In his work, Pierce made the following assumptions:

1. The modulation of both the electron velocity and the current on the beam (so called a.c. components) are small compared to the average or unperturbed velocity and current.

2. The beam is thought of as a continuous medium (electron jelly) with no internal stress and a unique volumetric force acting along it, namely the one resulting from the axial component of the electric

   eld associated to the signal on the waveguide.

3. The action of the beam onto the waveguide amounts to a shunt current instantaneously induced on the line. This current is equal in absolute value and opposite to the current on the beam.

Under these assumptions, Pierce's model can be described by the following system of equations:

$$\begin{cases} \partial_z I = -C\partial_t V - \partial_z I_B, \quad \partial_z V = -L\partial_t I. \\ {\partial_t}^2 I_b + 2u_0 \partial_t \partial_z I_b + {u_0}^2 \partial_z^2 I_b = -\sigma \frac{e}{m} \rho_0 \partial_t \partial_z V. \end{cases} \tag{1.1}$$

The Pierce model is the simplest one-dimensional model of TWT that accounts for the RF signal amplification, energy extraction from the e-beam and its conversion into microwave radiation. The Pierce model consists of (i) an ideal linear representation of the e-beam and (ii) a lossless transmission line (TL) representing a waveguide structure. The transmission line is assumed to be homogeneous, that is with uniformly distributed capacitance and

inductance. This model captures significant features of the wave amplification and the beam-wave energy transfer remarkably well, and is still used for basic design estimates.

1.4 Lagrangian formulation of Pierce's model

Development of the multi-transmission line-beam (MTLB) theory is motivated by the ease in which a Lagrangian framework of the system gives insight into the amplification regimes and energy transfer in TWT-systems. In 2013, Figotin and Reyes constructed a Lagrangian field theory generalizing and extending the Pierce theory to the case of possibly inhomogeneous MTL coupled to the ebeam [10]. The e-beam was treated there essentially in the same vein as Pierce's model. The construction of a Lagrangian framework allowed for keeping the simplicity and constructiveness of the Pierce model, while allowing for more complex slow-wave structures.

The Lagrangian formulation of the TLB system is given by

$$\mathscr{L}(z, \partial_t Q, \partial_z Q, \partial_t q, \partial_z q) = \frac{L}{2}(\partial_t Q)^2 - \frac{1}{2}C^{-1}(\partial_z Q + \partial_z q)^2 + \frac{\xi}{2}(\partial_t q + u_0 \partial_z q)^2. \tag{1.2}$$

The corresponding Euler-Lagrange equations are:

$$\begin{cases} L\partial_t^2 Q - \partial_z[C^{-1}\partial_z](Q+q) = 0; \\ \xi(\partial_t + u_0\partial_z)^2 q - \partial_z[C^{-1}\partial_z](Q+q) = 0, \end{cases} \tag{1.3}$$

where

$$\xi = \frac{4\pi}{\omega_p^2 \sigma} = \frac{m}{\sigma e \rho_0} > 0. \tag{1.4}$$

The Lagrangian formulation of the TLB is then easily generalized to the MTLB Lagrangian formulation. Let $V(z,t) = \{V_i(z,t)\}_{i=1}^n$ denote the n-dimensional vector-column of voltages on the first n conductors with respect to the ground and $I(z,t) = \{I_i(z,t)\}_{i=1}^n$ the vector-column of currents flowing on them and set:

$$Q(z,t) = \{Q_i(z,t)\}_{i=1}^n, \;\; Q_i(z,t) = \int^t I_i(z,s)\, ds. \tag{1.5}$$

Let $L = L(z), C = C(z)$ denote the positive, symmetric $n \times n$ matrices of self- and mutual inductance and capacity. We view the Lagrangian of the coupled system as $\mathscr{L} = \mathscr{L}_{Tb} + \mathscr{B}$, where $\mathscr{L}_{Tb}$ represents the Lagrangian of the MTL and $\mathscr{L}_B$ represents the Lagrangian of the beam itself:

$$\mathscr{L}_B = \frac{\xi}{2}(\partial_t q + u_0 \partial_z q)^2. \tag{1.6}$$

Then, the Lagrangian of the coupled system is given by:

$$\mathscr{L} = \frac{1}{2}\{(\partial_t Q, L\partial_t Q) - (\partial_z Q + \partial_z qB, C^{-1}[\partial_z Q + \partial_z qB])\} + \frac{\xi}{2}(\partial_t q + u_0 \partial_z q)^2, \tag{1.7}$$

where $(\ ,\ )$ stands for the scalar product in $\mathbb{R}^n$ and B is the n-dimensional vector-column with all components being the unity, i.e.

$$B = (1, 1, \ldots, 1)^T. \tag{1.8}$$

The corresponding second-order Euler-Lagrange equations are given by:

$$\begin{cases} L\partial_t^2 Q - \partial_z[C^{-1}(\partial_z Q + \partial_z qB)] = 0; \\ \xi[\partial_t^2 q + tu_0\partial_t\partial_z q + u_0^2\partial_z^2 q] - (B^T, \partial_z[C^{-1}(\partial_z Q + \partial_z qB)]) = 0. \end{cases} \tag{1.9}$$

In short, the Lagrangian approach allowed for extension of the Pierce model in two directions: a) replacing the transmission line by a multi-transmission line (MTL) and b) removing the homogeneity assumption, thus considering general nonhomogeneous systems consisting of a multi-transmission line (MTL) coupled to an electron beam. This system is referred to as a MTLB system. Extension to multiple transmission lines is motivated by the fact that general MTLs can approximate with desired accuracy real wave-guide structures which can be homogeneous (uniform) as well as inhomogeneous. Again, in [10], the electron beam was treated essentially the same as in Pierce's model. however, in the following chapter, this assumption is generalized by representing the electron beam by a finite number of electron streams.

Chapter 2 describes the multi-stream e-beam (MSB), the model used in our studies for the remainder of the text. Construction of the MSB is described in complete detail in [9], while here we only briefly summarize its key features and assumptions.

Chapter 2

Summary of the MSB model

Generalization of the MTLB system to the MSB system allows for analysis of several phenomena including, for example, space charge effects and high frequency instability regimes in the coupled system. For our purposes here, the most significant feature of the MSB system is its ability to model system instability in the uncoupled system. As we will see in Chapter 4, exponentially growing instability is absent in the single-stream uncoupled case, but present in the two-stream uncoupled system.

In this chapter we formulate the essential definitions and notation used in the remainder of the text as well as the Lagrangian formulation of the MSB system.

2.1 Parameters and notation for MSB

Here, we provide the relevant quantities and notation used throughout the text. We assume the electron beam consists of a finite number of n_B electron streams, indexed by s with $1 \leq s \leq n_B$. We assume the state of the electron beam can be viewed as a small perturbation of a steady state described by a constant (independent of space and time) number of electron

densities $\mathring{n}_s$ and steady velocities $\mathring{v}_s$ satisfying

$$0 < \mathring{v}_1 < \ldots < \mathring{v}_{n_B}. \tag{2.1}$$

The state of the beam is described by the corresponding pairs of small perturbations, $n_s = n_s(t,z)$ and $v_s = v_s(t,z)$ of the stationary state. We define the *electron stream parameters* by

$$\beta_s = \frac{\sigma_B}{4\pi}{\omega_{ps}}^2, \;\; \omega_{ps}^2 = \frac{4\pi \mathring{n}_s e^2}{m}, \;\; 1 \leq s \leq n_B. \tag{2.2}$$

where $e > 0$ is the electron charge, m is the electron mass, and ${\omega_{ps}}^2$ are plasma frequencies, and σ_B is the area of the cross-section of the beam. We also write the normalized electron stream parameters by

$$\hat{\beta}_s = \frac{\beta_s}{\overline{\beta}}, \; \overline{\beta} = \sum_{s=1}^{n_B} \beta_s. \tag{2.3}$$

To model the electron beam interacting with the MTL, we use the following column vector of *stream charges*:

$$q(z,t) = \{q_s(z,t)\}_{s=1}^{n_B}. \tag{2.4}$$

As for the MTL, we assume it consists of n_T transmission lines and use the following n_T-dimensional column vector of charges:

$$Q(z,t) = \{Q_j(z,t)\}_{j=1}^{n_T}. \tag{2.5}$$

We use $n_T \times n_T$ symmetric, positive-definite inductance and capacitance matrices $L = L(z)$

and $C = C(z)$ to model material properties of the MTL.

Vector representations of quantities appearing in the system Lagrangian are as follows:

$$q = \begin{bmatrix} q_1 \\ \vdots \\ q_{n_B} \end{bmatrix}, \quad \psi_B = \begin{bmatrix} \frac{\hat{\beta}_1}{(u-\check{v}_1)^2} \\ \vdots \\ \frac{\hat{\beta}_{n_B}}{(u-\check{v}_{n_B})^2} \end{bmatrix} \quad Q = \begin{bmatrix} Q_1 \\ \vdots \\ Q_{n_T} \end{bmatrix}. \tag{2.6}$$

To couple the e-beam to n_T-many transmission lines, we define the *coupling vector* with constant entries b_s for $1 \leq s \leq n_T$:

$$b = \begin{bmatrix} b_1 \\ b_2 \\ \vdots \\ b_{n_T} \end{bmatrix}, \quad 0 \leq b_s \leq 1, \tag{2.7}$$

where $b_s = 0$ means that the e-beam is not coupled to the s-th transmission line and $b_s = 1$ means that the e-beam is fully coupled to it.

Now we can define the *MTL parameters* by

$$\theta_s = w_s^2 \left| \left(e_s, L^{1/2} b \right) \right|^2, \quad \bar{\theta} = \sum_{s=1}^{n_T} \theta_s. \tag{2.8}$$

The normalized parameters are given by

$$\hat{\theta} = \frac{\theta_s}{\bar{\theta}}, \quad \sum_{s=1}^{n_T} \hat{\theta} = 1, \tag{2.9}$$

where $1 \leq s \leq n_T$.

2.2 Lagrangian formulation for MSB model

The Lagrangian framework for the TWT-system is given by:

$$\mathscr{L}_{TB} = \mathscr{L}_{Tb} + \mathscr{L}_B, \tag{2.10}$$

where $\mathscr{L}_{Tb}$ represents the Lagrangian of the MTL and $\mathscr{L}_B$ represents the Lagrangian of the beam. Each of these components are defined by:

$$\begin{aligned}
\mathscr{L}_{Tb}(\{\partial_t Q_j, \partial_z Q_j\}) &= \frac{1}{2}(\partial_t Q, L\partial_t Q) - \frac{1}{2}(\partial_z Q + \partial_z \bar{q} b, C^{-1}[\partial_z Q + \partial_z \bar{q} b]), \\
\mathscr{L}_B(\{q_s, \partial_t q_s, \partial_z q_s\}) &= \sum_{s=1}^{n_B} \frac{1}{2\beta_s}(\partial_t q_s + \mathring{v}_s \partial_z q_s)^2 - \frac{2\pi}{\sigma_B}\bar{q}^2, \quad \bar{q} = \sum_{s=1}^{n_B} q_s.
\end{aligned} \tag{2.11}$$

Here, $(\cdot,\cdot)$ denotes the scalar product in the Euclidean space $\mathbb{R}^{n_T}$, the parameters β_s are as above, and b is the n_T-dimensional coupling column vector defined above. The constant R_{SC} denotes the *plasma frequency reduction factor*.

The Euler-Lagrange equations associated with the Lagrangian eq. (2.10) and eq. (2.11) above are the following system of second order equations:

$$\begin{aligned}
L\partial_t^2 Q - \partial_z[C^{-1}(\partial_z Q + b\partial_z \bar{q})] = 0, \;\; \bar{q} = \sum_{s=1}^{n_B} q_s, \\
\frac{1}{\beta_s}(\partial_t + \mathring{v}_s\partial_z)^2 q_s + \frac{4\pi}{\sigma_B}\bar{q} - (b, \partial_z[C^{-1}(\partial_z Q + b\partial_z \bar{q})]) = 0, \;\; 1 \le s \le n_B.
\end{aligned} \tag{2.12}$$

Taking the Fourier transform in the time and space variables t and z, respectively, yields:

$$\begin{aligned}
(k^2 C^{-1} - \omega^2 L)\hat{Q} + k^2 C^{-1} b\hat{\bar{q}} = 0, \\
\frac{4\pi}{\sigma_B}[\hat{\bar{q}} - \omega_{ps}^{-2}(\omega - \mathring{v}_s k)^2 \hat{q}_s] + k^2[(b, C^{-1}b)\hat{\bar{q}} + (b, C^{-1}\hat{Q})] = 0,
\end{aligned} \tag{2.13}$$

where ω and k denote the frequency and wave number, respectively. The vectors $\hat{Q} = \hat{Q}(\omega, k)$

and $\hat{q} = \hat{q}(\omega, k)$ are the Fourier transforms of the system vector variables $Q(t, z)$ and $q(t, z)$.

2.3 Characteristic equations for MSB

To analyze solutions of the above Euler-Lagrange equations, we will define three characteristic functions, each capturing various structural features of the MTLB system components. Our primary focus is to study mathematical properties of some of the characteristic functions associated with the e-beam and their solutions in the uncoupled system.

The first characteristic function associated with the e-beam is the *inverse characteristic function of the electron beam*, defined here as:

$$\Delta_B(u) = \sum_{i=1}^{n_B} \frac{\hat{\beta}_s}{(u - \mathring{v}_s)^2} = {1_B}^T \psi_B, \quad u = \frac{\omega}{k}. \tag{2.14}$$

where the $\hat{\beta}_s$ and $\mathring{v}_s$ are as above, 1_B denotes the n_B-dimensional constant column vector with entries identically 1, and u is the complex valued phase velocity.

We will also consider the frequency dependent *space charge function* h_ω, as it relates to eq. (2.16). It quantifies the debunching effects and is defined by:

$$h = h_\omega = \frac{4\pi {R_{sc}}^2}{\sigma_\beta \omega^2} = \frac{1}{\overline{\beta}\breve{\omega}^2}, \qquad \breve{\omega} = \frac{\omega}{{R_{sc}}^2 \overline{\omega_p}}. \tag{2.15}$$

Here, R_{sc} is the *plasma frequency reduction factor* which accounts for the finite domain of the beam, geometric features of the MTL, and debunching effects.

The other characteristic equation associated with the e-beam is given by:

$$D_B(u) = u^{-2}\Delta_B(u) = \frac{1}{\breve{\omega}^2}. \tag{2.16}$$

We refer to the above equation as the *normalized characteristic function of the e-beam* or the *normalized e-beam function*.

While we only present results concerning the uncoupled system in this text, for completeness we give the definitions of the characteristic function associated with the MTL. The *MTL characteristic function* is given by:

$$\Delta_T(u) = u^2 \sum_{s=1}^{n_T} \frac{\hat{\theta}_s}{{\omega_s}^2 - u^2}. \tag{2.17}$$

When coupling the e-beam to the MTL, we obtain the TWT-system. Consequently, combining the respective characteristic functions we obtain the following *TWT characteristic equation* for phase velocity u:

$$\overline{\gamma} u^{-2}\Delta_T(u) + u^{-2}{\Delta_B}^{-1}(u) = \frac{1}{\breve{\omega}^2}. \tag{2.18}$$

where $\overline{\gamma} = \overline{\theta\beta}$ represents the *MTLB system parameter*.

When $\overline{\gamma} = 0$, the above characteristic equation reduces to eq. (2.16) and represents the uncoupled system, which is the subject of our studies here.

In what follows, we analyze the zero set of eq. (2.14), solutions to eq. (2.16) in the two-stream case ($n_B = 2$), and in particular, those solutions which give rise to system instability.

2.4 Eigenmodes of the system

The system eigenmodes of the MSB system are of the form:

$$Q(z,t) = \hat{Q}(k,\omega)e^{-i(\omega t - kz)}, \quad q(z,t) = \hat{q}(k,\omega)e^{-i(\omega t - kz)}, \tag{2.19}$$

where $\hat{Q}$ and $\hat{q}$ are the Fourier transforms of Q and q, respectively. As amplification in the TWT is a result of instability in the MSB system, we are particularly interested in spatially exponentially growing eigenmodes, i.e. those eigenmodes that correspond to non-real wave numbers k. Moreover, using the dispersion relation $u = \omega/k$, we see that u is non-real if and only if k is non-real.

Using the notation in the previous section and the characteristic functions defined there, we have the following closed form representation of $\hat{Q}(u)$ and $\hat{q}(u)$:

$$\hat{q} = a_0\psi_B(u), \hat{q}_s = a_0[\psi_B]_s(u) = a_0\frac{\hat{\beta}_s}{(u - \mathring{v}_s)^2}, \text{ for } 1 \leq sleqn_B, \tag{2.20}$$

and

$$\hat{Q} = -a_0\Delta_B(u)(C^{-1} - u^2L)^{-1}C^{-1}b, \tag{2.21}$$

where the phase velocity u is a solution to eq. (2.18). Thus, non-real solutions u to the TWT characteristic equation correspond to exponentially growing eigenmodes and consequently, system instability.

One of our primary interests is understanding the transition from an unstable to stable (oscillatory) TWT system in the two-stream case, which we describe in chapter 4. In the next chapter we study the zero set of eq. (2.14), that is, the phase velocities u for which $\omega = 0$.

Chapter 3

The zero set of the inverse characteristic e-beam function

While we are primarily concerned with the two-stream MSB system, in this chapter we establish a more general fact about the inverse characteristic function Δ_B given by eq. (2.14) for any finite number of streams n_B. More specifically, we show that for almost every choice of positive beam parameters β_s, the zeros of Δ_B are distinct. Moreover, in the proof we see that in the two-stream case, no further conditions on β_1 and β_2 are needed, i.e. for any positive β_1 and β_2, the zeros of Δ_B are always distinct when $n_B = 2$.

In general, one can show that the zero set of a nontrivial, real-valued polynomial in several variables has Lebesgue measure zero and apply this result to the discriminant of the characteristic function Δ_B. Thus one can conclude that if its discriminant is not identically 0, then the roots of Δ_B are distinct almost everywhere; however, in practice, showing that the discriminant of a general polynomial is nontrivial is not easy to do explicitly. Instead, in section 3.1 we formulate our main result on the nondegeneracy of the roots of Δ_B and provide an alternative line of argument using induction and Rouche's theorem to show that

the roots of eq. (2.14) are distinct for almost every choice of β_s, $1 \leq s \leq n_B$. In the last section, we provide a detailed analysis and computation in the $n_B = 2, 3$ cases and provide explicit conditions on the parameters β_s to guarantee distinct roots of Δ_B.

3.1 Main result on the nondegeneracy of roots

For some electron stream parameters β_s, the roots of eq. (2.14) may not be distinct, in which case we say the roots are *degenerate*. We claim that this is not the case in general.

Theorem 3.1.1 (Nondegeneracy of the roots of Δ_B)**.** Let n_B be a positive integer, fix $0 < \mathring{v}_1 < \ldots < \mathring{v}_{n_B}$ and denote

$$\Delta_B(u) = \sum_{s=1}^{n_B} \frac{\beta_s}{(u - \mathring{v}_s)^2}. \tag{3.1}$$

Let $B = \{(\beta_1, \ldots, \beta_{n_B}) \in \mathbb{R}^{n_B} : \beta_s > 0, \text{ for } 1 \leq s \leq n_B, \Delta_B(u) = 0 \text{ has repeated roots}\}$. Then the Lebesgue measure of B (in $\mathbb{R}^{n_B}$) is zero.

Proof. We first note that the roots of $\Delta_B(u) = 0$ are precisely the roots of the polynomial equation

$$p(u) = \sum_{i=1}^{n_B} \beta_i \prod_{j \neq i} (u - \mathring{v}_j)^2 = 0. \tag{3.2}$$

Now, p is a polynomial of degree $2(n_B - 1)$, so it has $2(n_B - 1)$ roots. Moreover, since each of β_s are positive, the summands $\frac{\beta_s}{(u-\mathring{v}_s)^2}$ are also positive, so the roots of $\Delta_B(u)$ are all non-real. Moreover, this also means that the poles of $\Delta_B(u)$ are different from the roots of $\Delta_B(u)$ (and hence the roots of $p(u)$), since the poles of $\Delta_B(u)$ are the fixed real values $\mathring{v}_1, \ldots, \mathring{v}_{n_B}$.

We proceed to prove the theorem by induction. When $n_B = 2$,

$$\Delta_{B,2}(u) = \frac{\beta_1}{(u - \mathring{v}_1)^2} + \frac{\beta_2}{(u - \mathring{v}_2)^2}. \tag{3.3}$$

Rationalizing $\Delta_{B,2}$ and equating it with zero yields the polynomial equation $p(u) = (\beta_1 + \beta_2)u^2 - 2(\beta_1\mathring{v}_2 + \beta_2\mathring{v}_2)u + (\beta_1\mathring{v}_2^2 + \beta_2\mathring{v}_1^2) = 0$. Computing the discriminant of p, we have

$$discrim_p = -4(\mathring{v}_1 - \mathring{v}_2)^2\beta_1\beta_2, \tag{3.4}$$

which is nonzero if neither β_1 nor β_2 is zero. Thus, since β_1, β_2 are assumed to be positive, $B_2 = \{(\beta_1, \beta_2) \in \mathbb{R}^2 : \Delta_{B,2} = 0 \text{ has repeated roots}\} = \emptyset$, and hence B_2 has measure 0.

Inductively, assume that the Lebesgue measure of

$$\tilde{B} = \{(\beta_2, \ldots, \beta_{n_B}) \in \mathbb{R}^{n_B - 1} : \beta_s > 0 \text{ for } 2 \leq s \leq n_B, g(u) = 0 \text{ has repeated roots}\} \tag{3.5}$$

in $\mathbb{R}^{n_b - 1}$ is zero, where

$$g(u) = \sum_{s=2}^{n_B} = \frac{\beta_s}{(u - \mathring{v}_s)^2}. \tag{3.6}$$

.

Fix any $(\beta_2, \ldots, \beta_{n_B}) \notin \tilde{B}$, i.e. fix a set of parameters β_s for $2 \leq s \leq n_B$ for which the roots of g are distinct. Denote these roots by $z_1, \ldots z_{2(n_B - 2)}$. To prove the result, we use Rouche's Theorem (see Theorem A.1.1 in the Appendix).

Since the roots of g are distinct, for each z_i, choose a small disk D_i containing z_i so that $D_j \cap D_i = \emptyset$ if $i \neq j$. Moreover, choose the disks small enough so that none of the poles $\mathring{v}_1, \ldots, \mathring{v}_{n_B}$ are in any of the disks D_i. This can be done because the roots z_i of $\Delta_B(u)$ are non-real, but the poles v_i are real.

Fix $\hat{\beta} > 0$ and denote $f(u) = \frac{\hat{\beta}}{(u-\tilde{v}_1)^2}$. For each of the disks D_i above, choose K_i so large that $|K_i g| > |f|$ on the boundary of D_i. Then take $K = \max K_i$, so that $|Kg| > |f|$ on each D_i. By Rouche's theorem, the difference in zeros and poles of $f + Kg$ and Kg are the same in each D_i. Now, since the disks D_i contain exactly one zero and no poles of $\Delta_B(u)$, we know that $f + Kg$ and Kg have exactly one root in each D_i. Note that $f + Kg$ also has the same number of roots as g on D_i, since $g = 0$ exactly when $Kg = 0$.

By the above, we have accounted for $2(n_B - 2)$ distinct roots of $f + Kg$, but $f + Kg$ is a polynomial of degree $2(n_B-1)$. Now, since each summand of $f+Kg$ is positive, if $f+Kg = 0$, every root must be complex. Thus, the remaining two roots of $f+Kg$ are complex and must be complex conjugates. So the roots of $f + Kg$ are distinct.

Now, taking $\beta_1 = \hat{\beta}/K$, the argument above implies that for $(\beta_1, \ldots, \beta_{n_B}) \in \mathbb{R}^{n_B}$, the roots of $\Delta_B(u)$ are distinct, since $\Delta_B(u) = 0$ exactly when $K\Delta_B(u) = 0$ and $K\Delta_B(u) = f + Kg$.

The argument above holds for any choice of $(\beta_2, \ldots, \beta_{n_B}) \notin \tilde{B}$. Thus for any $\hat{\beta} > 0$, the parameters $(\beta_1, \ldots, \beta_{n_B})$ will produce repeated roots of $\Delta_B(u)$ if and only if $(\beta_2, \ldots, \beta_{n_B}) \in \tilde{B}$.

Let $B = \{(\beta_1, \ldots, \beta_{n_B}) \in \mathbb{R}^{n_B} : \beta_s > 0, \Delta_B(u) \text{ has repeated roots } \}$ and m_k denote the Lebesgue measure in $\mathbb{R}^k$. We have:

$$m_{n_B}(B) = \int_{\mathbb{R}} m_{n_B-1}(B_x)\, dm_1(x) = \int_{\mathbb{R}} 0\, dm_1(x) = 0, \tag{3.7}$$

where $B_x = \{(\beta_2, \ldots, \beta_{n_B}) : (x, \beta_2, \ldots, \beta_{n_B}) \in B\}$. □

3.2 Analysis for the two-stream and three-stream cases

While $discrim_p$ is a polynomial of the parameters β_i, v_i for $1 \leq i \leq n_B$, for simplicity, we denote $\overline{\beta} = (\beta_2, \ldots \beta_{n_B}, \mathring{v}_1, \ldots, \mathring{v}_{n_B})$, so that we may view the discriminant as a polynomial in $\beta_1, \overline{\beta}$:

$$discrim_p(\beta_1, \overline{\beta}) = \sum_{k=1}^{3n-5} c_k(\overline{\beta})\beta_1^k. \tag{3.8}$$

We analyze in detail the cases when $n_B = 2, 3$ in section 3.2.1 and section 3.2.2. Moreover, we find explicit conditions on $0 < \beta_s$ for $1 \leq s \leq n_B$ that guarantee $discrim_p = 0$, i.e., that guarantee that the roots of $p(u)$ are distinct.

3.2.1 The two-stream case

When $n_B = 2$ we have,

$$\Delta_B(u) = \frac{\beta_1}{(u - \mathring{v}_1)^2} + \frac{\beta_2}{(u - \mathring{v}_2)^2}, \tag{3.9}$$

and

$$p(u) = (\beta_1 + \beta_2)u^2 - 2(\beta_1\mathring{v}_2 + \beta_2\mathring{v}_2)u + (\beta_1\mathring{v}_2^2 + \beta_2\mathring{v}_1^2). \tag{3.10}$$

Since p is a polynomial of degree 2, we expect the discriminant of p to be a polynomial in β_1 of degree $3(2) - 5 = 1$. Indeed,

$$\begin{aligned} discrim_p(\beta_1, \overline{\beta}) &= 4(\beta_1\mathring{v}_2 + \beta_2\mathring{v}_2)^2 - 4(\beta_1 + \beta_2)(\beta_1\mathring{v}_2^2 + \beta_2\mathring{v}_1^2) \\ &= (-4(\mathring{v}_1 - \mathring{v}_2)^2\beta_2)\beta_1. \end{aligned} \tag{3.11}$$

So $c_1(\overline{\beta}) = -4(\mathring{v}_1 - \mathring{v}_2)^2\beta_2$. In this case, we see that $discrim(p) = 0$ exactly when $\mathring{v}_1 = \mathring{v}_2$ or β_1 or β_2 is zero. Since we have assumed that $0 < \mathring{v}_1 < \mathring{v}_2$ and that $\beta_1, \beta_2 > 0$, $discrim_p \neq 0$ for any choice of positive β_s. Thus, in the two-stream case, the zeroes of Δ_B are always distinct.

Computing the roots of Δ_B in the $n_B = 2$ explicitly, we obtain the complex conjugate roots u_0 and $\bar{u_0}$ given by:

$$u_0 = \hat{\beta}_2(\mathring{v}_1 - \mathring{v}_2)\left(1 \pm i\sqrt{\hat{\beta}_1/\hat{\beta}_2}\right). \tag{3.12}$$

3.2.2 The three-stream case

Now, for $n_B = 3$, we have:

$$\Delta_B(u) = \frac{\beta_1}{(u - \mathring{v}_1)^2} + \frac{\beta_2}{(u - \mathring{v}_2)^2} + \frac{\beta_3}{(u - \mathring{v}_3)^2} \tag{3.13}$$

and

$$\begin{aligned} p(u) = {} & (\beta_1 + \beta_2 + \beta_3)u^4 + ((-2\beta_2 - 2\beta_3)\mathring{v}_1 + (-2\beta_1 - 2\beta_3)\mathring{v}_2 - 2\mathring{v}_3(\beta_1 + \beta_2))u^3 \\ & + ((\beta_2 + \beta_3)\mathring{v}_1^2 + (4\mathring{v}_2\beta_3 + 4\mathring{v}_3\beta_2)\mathring{v}_1 + (\beta_1 + \beta_3)\mathring{v}_2^2 + 4\beta_1\mathring{v}_3\mathring{v}_2 + \mathring{v}_3^2(\beta_1 + \beta_2))u^2 \\ & + ((-2\mathring{v}_2\beta_3 - 2\mathring{v}_3\beta_2)\mathring{v}_1^2 + (-2\mathring{v}_2^2\beta_3 - 2\mathring{v}_3^2\beta_2)\mathring{v}_1 - 2\mathring{v}_3\beta_1\mathring{v}_2(\mathring{v}_2 + \mathring{v}_3))u \\ & + (\mathring{v}_2^2\beta_3 + \mathring{v}_3^2\beta_2)\mathring{v}_1^2 + \beta_1\mathring{v}_3^2\mathring{v}_2^2. \end{aligned} \tag{3.14}$$

a polynomial of degree 4 in u. It's discriminant, $discrim_p(\beta_1, \overline{\beta})$ is a polynomial of degree 4 in β_1, with coefficients:

$$\begin{aligned}
c_4(\overline{\beta}) &= 16(\mathring{v}_2 - \mathring{v}_3)^8(\mathring{v}_1 - \mathring{v}_3)^2(\mathring{v}_1 - \mathring{v}_2)^2\beta_2\beta_3 \\
c_3(\overline{\beta}) &= 48(\mathring{v}_2 - \mathring{v}_3)^6(\mathring{v}_1 - \mathring{v}_3)^2(\mathring{v}_1 - \mathring{v}_2)^2(\beta_2(\mathring{v}_1 - \mathring{v}_3)^2 + \beta_3(\mathring{v}_1 - \mathring{v}_2)^2)\beta_2\beta_3 \\
c_2(\overline{\beta}) &= 48(\mathring{v}_2 - \mathring{v}_3)^4(\mathring{v}_1 - \mathring{v}_3)^2(\mathring{v}_1 - \mathring{v}_2)^2(\beta_2^2(\mathring{v}_1 - \mathring{v}_3)^4 - 7\beta_2\beta_3(\mathring{v}_1 - \mathring{v}_3)^2(\mathring{v}_1 - \mathring{v}_2)^2 \\
&\quad + (\mathring{v}_1 - \mathring{v}_2)^4\beta_3^2)\beta_2\beta_3 \\
c_1(\overline{\beta}) &= 16(\mathring{v}_2 - \mathring{v}_3)^2(\mathring{v}_1 - \mathring{v}_3)^2(\mathring{v}_1 - \mathring{v}_2)^2(\beta_2(\mathring{v}_1 - \mathring{v}_3)^2 + \beta_3(\mathring{v}_1 - \mathring{v}_2)^2)^3\beta_2\beta_3.
\end{aligned} \tag{3.15}$$

Notice that each c_k contains $(\mathring{v}_1 - \mathring{v}_2)^{k_1}(\mathring{v}_1 - v_3)^{k_2}(\mathring{v}_2 - \mathring{v}_3)^{k_3}$ for some positive integers k_1, k_2, k_3, and that $c_4(\overline{\beta})$ contains no other polynomial expressions involving the v_i. This implies that $c_4(\overline{\beta}) \neq 0$ for any $\beta_2, \beta_3 > 0$, since $0 < \mathring{v}_1 < \mathring{v}_2 < \mathring{v}_3$.

We denote

$$C = \{(\beta_1, \overline{\beta}) \in \mathbb{R}^6 : discrim_p(\beta_1, \overline{\beta}) = 0\}. \tag{3.16}$$

For fixed $\overline{\beta}$, we consider $C_{\overline{\beta}} = \{\beta_1 \in \mathbb{R} : (\beta_1, \overline{\beta}) \in C\}$. Then $m(C_{\overline{\beta}}) = 0$, because for fixed $\overline{\beta}$, as a polynomial in β_1, $discrim_p$, can have only finitely many roots. Thus, by Fubini's theorem,

$$m_6(C) = \int m(C_{\overline{\beta}})\, dm_5 = 0. \tag{3.17}$$

Now, having expressing $discrim_p$ as a polynomial in β_1 according to eq. (3.15) with coeffi-

cients c_i, we see that each coefficient can be thought of as

$$c_i = A(\mathring{v}_1 - \mathring{v}_2)^{k_1}(\mathring{v}_1 - v_3)^{k_2}(\mathring{v}_2 - v_3)^{k_3} g_i \tag{3.18}$$

where A is some integer and g_i is a polynomial in the parameters $\beta_2, \beta_3, \mathring{v}_1, \mathring{v}_2, \mathring{v}_2$. We will find precise conditions on the β_i to guarantee that each $c_i > 0$.

Since $0 < \mathring{v}_1 < \mathring{v}_2 < \mathring{v}_3$, we see that $c_i = 0$ if and only if $g_i = 0$. Take each $\beta_i > 0$. Then both g_1, g_3, and g_4 are all positive, so $c_1, c_3, c_4 > 0$. Viewing g_2 as a quadratic in β_3 and applying to quadratic formula, we see that $g_2 = 0$ if and only if

$$\beta_3 = \frac{7 \pm 3\sqrt{5}\beta_2}{2} \left(\frac{\mathring{v}_1 - v_3}{\mathring{v}_1 - \mathring{v}_2} \right)^2. \tag{3.19}$$

Since β_3 is positive, we see that in the $n_B = 3$ case, for any $\beta_1, \beta_2, \beta_3 > 0$ and

$$\beta_3 \neq \frac{7 + 3\sqrt{5}\beta_2}{2} \left(\frac{\mathring{v}_1 - v_3}{\mathring{v}_1 - \mathring{v}_2} \right)^2, \tag{3.20}$$

$g_i > 0$. Thus, each $c_i > 0$, which implies that $discrim_p > 0$, i.e. p and Δ_B have distinct roots.

Chapter 4

Solutions to the e-beam characteristic function in the two-stream case

Our main equation of interest is the characteristic equation of the e-beam given by eq. (4.13) when $n_B = 2$. Depending on the value chosen for ω, solutions u to the characteristic equation can be real or non-real. Thus, we would like to analyze solutions near the critical point u_c at which solutions transition from unstable (non-real) to oscillatory (real). To do so, we introduce a change of variables that recasts the equation in terms of a new complex variable s, and consider solutions to $T_B(s) = \omega'^2$. We represent solutions s near the critical point s_c of T_B using a Puiseux series, which allows us to easily observe the dependence of solutions s on ω and the behavior of $\Im(s)$ for complex solutions $s(\omega)$.

In the following sections, we describe properties of the eq. (4.13) and the singularity behavior of solutions $u(\omega)$ near ω_c when the two streams merge. After a change of variables, we consider a new characteristic equation $T_B(s) = \omega'^2$ (eq. (4.29)) and use a Puiseux series to represent solutions near its critical point s_c. Lastly, we analyze the imaginary part of non-real solutions to eq. (4.29).

4.1 Properties of the characteristic function of the beam

The goal of this section is to study solutions to the normalized characteristic equation $D_B(u)$ associated with the electron beam when $n_B = 2$:

$$D_B(u) = \frac{1}{u^2 \Delta_B(u)} = \frac{1}{\omega^2} \tag{4.1}$$

where $u = \omega/k$ is complex, k is complex, and ω is real, and

$$\Delta_B(u) = \frac{\beta_1}{(u - \mathring{v}_1)^2} + \frac{\beta_2}{(u - \mathring{v}_2)^2}. \tag{4.2}$$

We want to study complex solutions $u = u(\omega)$ to the above characteristic equation that are not real, since these solutions provide for an instability regime in the MTLB system. However, it is beneficial to our analysis of non-real solutions u to observe some properties of $D_B(u)$ when u is real. For $u \in \mathbb{R}$, the graph of $D_B(u)$ is given below.

Function $D_B(u)$ of the electron beam for real u.

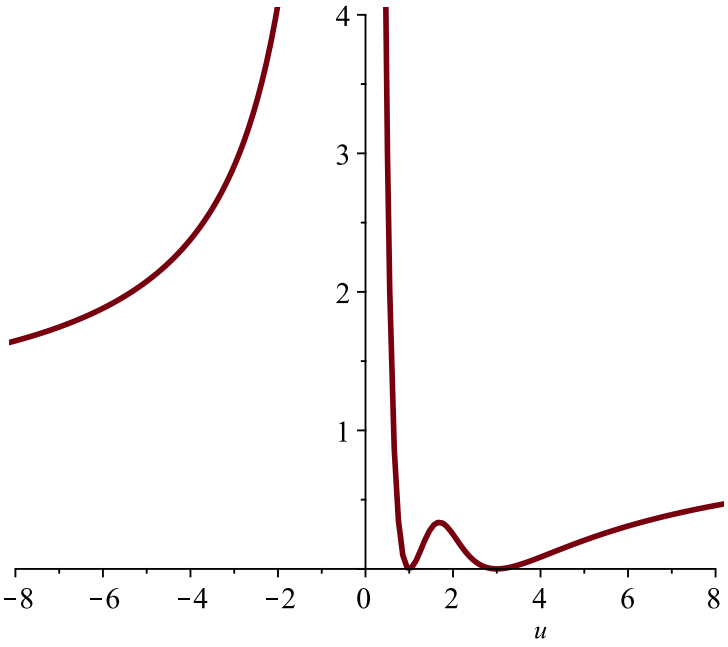

From the graph it is easy to see that D_B should have two zeros at $\mathring{v}_1, \mathring{v}_2$ and a critical point u_c in $(\mathring{v}_1, \mathring{v}_2)$. Moreover, D_B has a vertical asymptote at $u = 0$ and a horizontal asymptote at $y = 1$. We summarize these facts in the following theorem:

Theorem 4.1.1. Let $0 < \mathring{v}_1 < \mathring{v}_2$ and $\beta_1, \beta_2 \in \mathbb{R}$ so that $\beta_1 + \beta_2 = 1$. When $n_B = 2$, $D_B(u)$ always has the following properties:

1. $u = 0$ is a pole and $y = 1$ is a vertical asymptote,
2. $\mathring{v}_1, \mathring{v}_2$ are zeros of D_B, and
3. u_c is a real critical point in $(\mathring{v}_1, \mathring{v}_2)$ of D_B.

Proof. We can simplify D_B so that

$$D_B(u) = \frac{1}{u^2} \frac{1}{\frac{\beta_1}{(u-\mathring{v}_1)^2} + \frac{\beta_2}{(u-\mathring{v}_2)^2}} = \frac{(u-\mathring{v}_1)^2(u-\mathring{v}_2)^2}{u^2(\beta_1(u-\mathring{v}_2)^2 + \beta_2(u-\mathring{v}_1)^2}. \tag{4.3}$$

Thus D_B can be expressed as a rational function with degree four numerator and denominator. From here it is easy to see that

$$\begin{aligned} \lim_{u\to 0} D_B(u) &= +\infty \text{ and} \\ \lim_{|u|\to+\infty} D_B(u) &= \frac{1}{\beta_1 + \beta_2} = 1, \end{aligned} \tag{4.4}$$

which establishes 1. Moreover, $\mathring{v}_1$ and $\mathring{v}_2$ are zeros of the numerator of $D_B(u)$, and hence D_B which establishes 2.

Differentiating D_B and using $\beta_1 + \beta_2 = 1$, we obtain:

$$D'_B(u) = \frac{2(u-\mathring{v}_1)(u-\mathring{v}_2)(\beta_2\mathring{v}_2(u-\mathring{v}_1)^3 + \beta_1\mathring{v}_1(u-\mathring{v}_2)^3)}{u^3(\beta_2(u-\mathring{v}_1)^2 + \beta_1(u-\mathring{v}_2)^2)^2} \tag{4.5}$$

Thus the remaining critical points of D_B (i.e. critical points other than $\mathring{v}_1, \mathring{v}_2$) come from roots of $\beta_2\mathring{v}_2(u-\mathring{v}_1)^3 + \beta_1\mathring{v}_1(u-\mathring{v}_2)^3$. Viewing this cubic polynomial as a sum of cubes, we conclude that we have a real critical point u_c of D_B which is the real root of the cubic polynomial. The other two roots of this polynomial will be complex conjugates. If

$$\beta_2\mathring{v}_2(u_c-\mathring{v}_1)^3 + \beta_1\mathring{v}_1(u_c-\mathring{v}_2)^3 = [\sqrt[3]{\beta_2\mathring{v}_2}(u_c-\mathring{v}_1)]^3 + [\sqrt[3]{\beta_1\mathring{v}_1}(u_c-\mathring{v}_2)]^3 = 0, \tag{4.6}$$

then factoring yields

$$(\sqrt[3]{\beta_2\mathring{v}_2}(u_c-\mathring{v}_1) + \sqrt[3]{\beta_1\mathring{v}_1}(u_c-\mathring{v}_2)) = 0, \tag{4.7}$$

and

$$((\sqrt[3]{\beta_2\mathring{v}_2}(u_c-\mathring{v}_1))^2 - \sqrt[3]{\beta_1\beta_2\mathring{v}_1\mathring{v}_2}(u_c-\mathring{v}_1)(u_c-\mathring{v}_2) + (\sqrt[3]{\beta_1\mathring{v}_1}(u_c-\mathring{v}_2))^2) = 0. \tag{4.8}$$

From the linear factor, we obtain:

$$\sqrt[3]{-\frac{\beta_2\mathring{v}_2}{\beta_1\mathring{v}_1}} = \frac{u_c-\mathring{v}_2}{u_c-\mathring{v}_1}, \tag{4.9}$$

from which we obtain the real critical point u_c:

$$u_c = \frac{\mathring{v}_1\sqrt[3]{\frac{-\beta_2\mathring{v}_2}{\beta_1\mathring{v}_1}} - \mathring{v}_2}{\sqrt[3]{\frac{-\beta_2\mathring{v}_2}{\beta_1\mathring{v}_1}} - 1} = \frac{\mathring{v}_1\sqrt[3]{\frac{\beta_2\mathring{v}_2}{\beta_1\mathring{v}_1}} + \mathring{v}_2}{\sqrt[3]{\frac{\beta_2\mathring{v}_2}{\beta_1\mathring{v}_1}} + 1}. \tag{4.10}$$

Note that since $\mathring{v}_1 < \mathring{v}_2$, we have

$$\mathring{v}_1\sqrt[3]{\frac{\beta_2\mathring{v}_2}{\beta_1\mathring{v}_1}} + \mathring{v}_1 < \mathring{v}_1\sqrt[3]{\frac{\beta_2\mathring{v}_2}{\beta_1\mathring{v}_1}} + \mathring{v}_2, \tag{4.11}$$

which implies that $\mathring{v}_1 < u_c$. Similarly, we have

$$\mathring{v}_1\sqrt[3]{\frac{\beta_2\mathring{v}_2}{\beta_1\mathring{v}_1}} + \mathring{v}_2 < \mathring{v}_2\sqrt[3]{\frac{\beta_2\mathring{v}_2}{\beta_1\mathring{v}_1}} + \mathring{v}_2, \tag{4.12}$$

so that $u_c < \mathring{v}_2$. Thus $u_c \in (\mathring{v}_1, \mathring{v}_2)$ as expected. □

4.2 Frequency dependent solutions to the characteristic equation and overview of the main problem

Our goal is to study solutions to the characteristic equation:

$$D_B(u) = 1/\omega^2. \tag{4.13}$$

More specifically, we want to study solutions to the above equation that lie in the interval $(\mathring{v}_1, \mathring{v}_2)$, since these can be real or non-real, depending on ω. Solutions to eq. (4.13) are precisely solutions to $D_B(u) - 1/\omega^2$, and after rationalizing, they are solutions to:

$$\frac{\omega^2(u-\mathring{v}_1)^2(u-\mathring{v}_2)^2 - u^2(\beta_1(u-\mathring{v}_2)^2 + \beta_2(u-\mathring{v}_1)^2)}{\omega^2u^2(\beta_1(u-\mathring{v}_2)^2 + \beta_2(u-\mathring{v}_1)^2} = 0. \tag{4.14}$$

Thus, after simplifying the numerator, we see that the solutions u to the characteristic equation $D_B(u) = 1/\omega^2$ are solutions to the quartic polynomial:

$$f_D(u) = (\omega^2-1)u^4 + ((-2(\mathring{v}_1+\mathring{v}_2)\omega^2 + 2(\beta_1\mathring{v}_2 + \beta_2\mathring{v}_1))u^3 \tag{4.15}$$

$$+ ((\mathring{v}_1^2 + 4\mathring{v}_1\mathring{v}_2 + \mathring{v}_2^2)\omega^2 - \beta_1\mathring{v}_2^2 - \beta_2\mathring{v}_1^2)u^2 \tag{4.16}$$

$$- 2\omega^2\mathring{v}_1\mathring{v}_2(\mathring{v}_1+\mathring{v}_2)u + \mathring{v}_1^2\mathring{v}_2^2\omega^2 = 0, \tag{4.17}$$

where we have used the condition $\beta_1 + \beta_2 = 1$ to simplify the leading coefficient. Moreover, when $\omega = 1$, the leading coefficient vanishes, resulting in a cubic polynomial. This agrees with what we expect from the graph above; in particular, we see that $D_B(u) = 1$ for some $u \in (0, \mathring{v}_1)$. More importantly, depending on the values chosen for ω (and provided that $\omega \neq 1$), f_D will have four real solutions or one pair of complex conjugate solutions and two real solutions.

Whether f_D and hence $D_B = 1/\omega^2$ yield non-real solutions is determined by the critical point u_c computed in the previous section. From the graph of D_B for real u, it is clear that if u_c denotes the critical point of D_B between $\mathring{v}_1$ and $\mathring{v}_2$ and ω_c satisfies $D_B(u_c) = 1/{\omega_c}^2$, for $\omega < \omega_c$, there should be two non-real solutions to $D_B(u) = \omega^2$.

Here we include a graphical representation showing the "branching point" at which solutions u to $D_B(u) = 1/\omega^2$ transition from non-real to real. The graph plots $(\Re(k), \omega)$ where $u = \omega/k$.

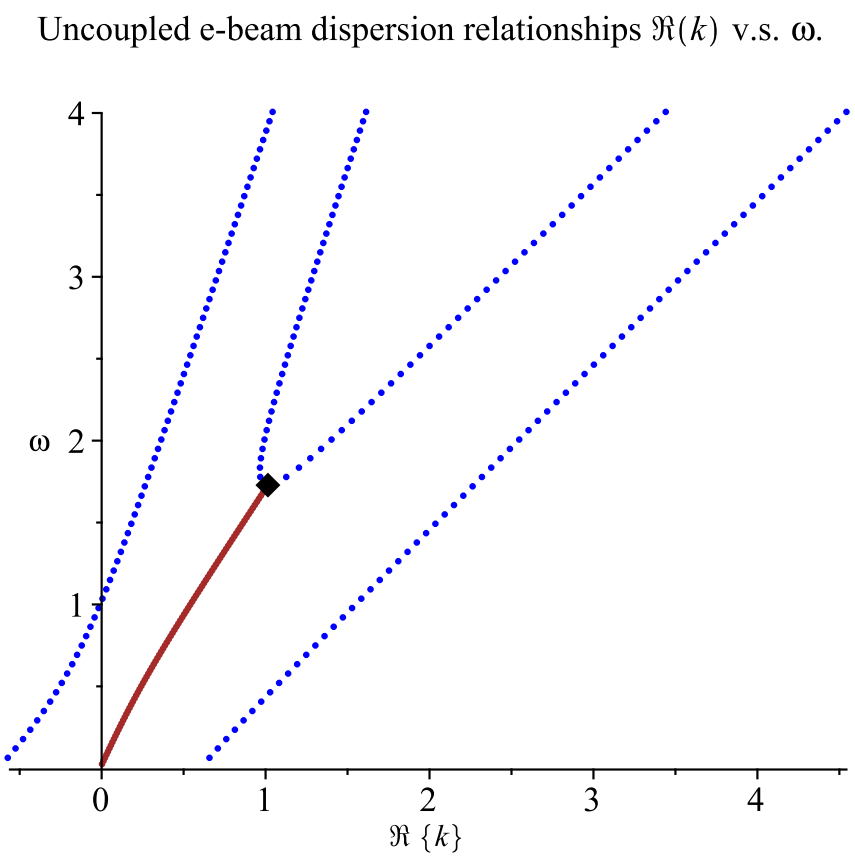

Here, the branching point, represented by a black diamond represents the frequency ω_c for which $D_B(u_c) = 1/{\omega_c}^2$. For a solution u, using $u = \omega/k$, we represent $\Re(k)$ with blue dotted lines and represent $\Im(k)$ with a solid brown line. We see that, as expected, for $\omega < \omega_c$ we have non-real solutions and for $\omega > \omega_c$, we have only real solutions.

4.3 Motivation for a change of variables: merging streams

Our goal is to study solutions u near the transition point u_c of the electron beam characteristic equation. To do so, we would like a representation of these solutions near ω_c that allows us to view their dependence on ω. Ultimately, we would like the representation to capture the behavior of the solutions $u(\omega)$ when the two streams merge ($\mathring{v}_2 \to \mathring{v}_1$). Unfortunately, in

its current form, the characteristic equation D_B has a singularity at ω when $\mathring{v}_2 \to \mathring{v}_1$. We summarize the singularity behavior in the following theorem:

Theorem 4.3.1. Let $0 < \mathring{v}_1 < \mathring{v}_2, \beta_1, \beta_2 \in \mathbb{R}$ so that $\beta_1 + \beta_2 = 1$ and let $\omega > 0$. As $\mathring{v}_2 \to \mathring{v}_1$, if u_c is the real critical point of D_B in $(\mathring{v}_1, \mathring{v}_2)$, then $\omega_c \to \infty$, where ω_c satisfies $D_B(u) = 1/{\omega_c}^2$.

Proof. Using the representation of u_c from eq. (4.10), we have:

$$\lim_{\mathring{v}_2 \to \mathring{v}_1} u_c = \lim_{\mathring{v}_2 \to \mathring{v}_1} \frac{\mathring{v}_1 \sqrt[3]{\frac{\beta_2 \mathring{v}_2}{\beta_1 \mathring{v}_1}} + \mathring{v}_2}{\sqrt[3]{\frac{\beta_2 \mathring{v}_2}{\beta_1 \mathring{v}_1}} + 1} = \mathring{v}_1. \tag{4.18}$$

Thus, we see that since D_B is continuous for all $u > 0$,

$$\lim_{\mathring{v}_2 \to \mathring{v}_1} D_B(u_c) = D_B(\mathring{v}_1) = 0, \tag{4.19}$$

and since $D_B(u_c) = 1/{\omega_c}^2$,

$$\lim_{\mathring{v}_2 \to \mathring{v}_1} \omega_c = \infty. \tag{4.20}$$

□

So as the two streams merge (i.e. $\mathring{v}_2 \to \mathring{v}_1$), we cannot simply represent solutions $u = u(\omega)$ as a convergent series, since ω is near ω_c, but $\omega_c \to \infty$.

4.3.1 One-stream vs. two-streams

One reason for this singularity can be seen in the following way: consider

$$D_{B,2}(u) = \frac{1}{u^2\left(\frac{\beta_1}{(u-\mathring{v}_1)^2} + \frac{\beta_2}{(u-\mathring{v}_2)^2}\right))} \tag{4.21}$$

$$= \frac{(u-\mathring{v}_1)^2(u-\mathring{v}_2)^2}{u^2(\beta_1(u-\mathring{v}_2)^2 + \beta_2(u-\mathring{v}_1)^2}, \tag{4.22}$$

and note that the numerator is a degree 4 polynomial. Now, as $\mathring{v}_2 \to \mathring{v}_1$ we have:

$$D_{B,2}(u) = \frac{(u-\mathring{v}_1)^2}{u^2(\beta_1+\beta_2)}, \tag{4.23}$$

a rational function with quadratic numerator. If we use the fact that $\beta_1 + \beta_2 = 1$, the above $D_{B,2}(u)$ characteristic function is precisely the one-stream $D_{B,1}(u)$ function:

$$D_{B,1}(u) = \frac{1}{u^2\frac{1}{(u-v)^2}}. \tag{4.24}$$

This collapse of power in the numerator accounts for the singularity behavior of u_c when $\mathring{v}_2 \to \mathring{v}_1$. More precisely, computing u_c in the one-stream case yields:

$$D'_{B,1}(u) = \frac{2(u-\mathring{v}_1)^2}{u^3}. \tag{4.25}$$

Thus, we see that $\mathring{v}_1$ is the only critical point of $D_{B,1}(u)$.

To visualize the solutions to $D_B(u)$ for a complex variable u, we use the dispersion relation $u = \omega/k$. The plots below show points $(\Re(k), \omega)$ where $u = \omega/k$ is a complex solutions to the characteristic equation. In the two-stream plot (left figure), the black diamond represents the instability node or "branching point" $(\Re(k), \omega_c)$ corresponding to u_c (that is, $D_B(u_c) = {\omega_c}^2$). As for the one-stream plot (right figure), as $\mathring{v}_2 \to \mathring{v}_1$ the critical point $u_c \to \mathring{v}_1$, and thus no

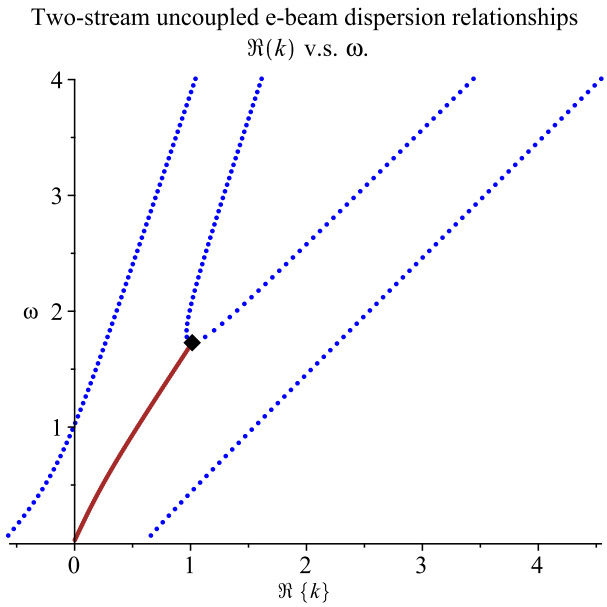

Figure 4.1: Two-stream dispersion relation.

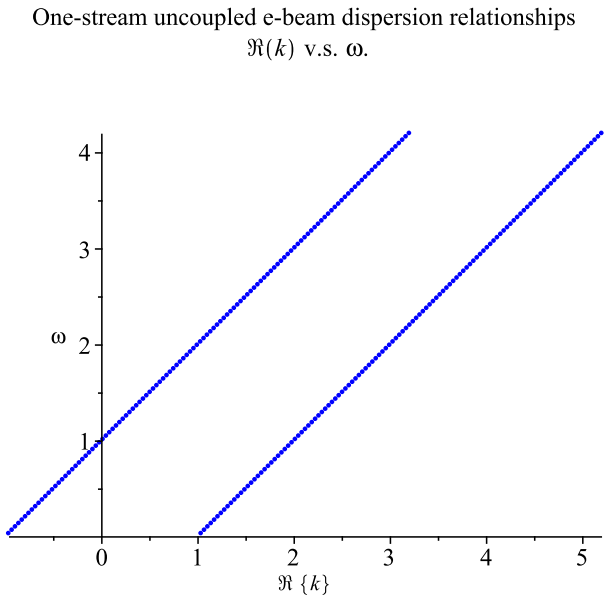

Figure 4.2: One-stream dispersion relation.

critical point exists occurs in $(\mathring{v}_1, \infty)$:

Here, we clearly see a distinct difference between the one-stream and two-stream cases: in the one-stream case, we have no branching point at which complex solutions transition to real solutions. As demonstrated in the previous section, when $\mathring{v}_2 \to \mathring{v}_1$, $\omega \to \infty$. Moreover, $\Re(k) \to \infty$ too. This is unexpected, since $\mathring{v}_2 \to \mathring{v}_1$ represents a two-stream MSB merging to one-stream, and in the one-stream case, we see no instability node. Intuitively, we expect the critical node $(\omega_c, \Re(k_c))$ corresponding to the critical point u_c in the $n_B = 2$ case to approach $(0, 0)$. However, this is not the behavior we observe which we discuss in the following section.

4.3.2 Merging streams graphs

Graphically, the collapse of power in eq. (4.13) that occurs as the streams merge can be seen when considering $u \in \mathbb{R}$. The plots below show $D_B(u)$ in the two-stream case as $\mathring{v}_1$ and $\mathring{v}_2$ merge. We also see that the critical point u_c of $D_B(u) \to \mathring{v}_1$ and $D_B(u_c) \to 0$, as expected.

Function $D_B(u)$ of the electron beam for various ε.

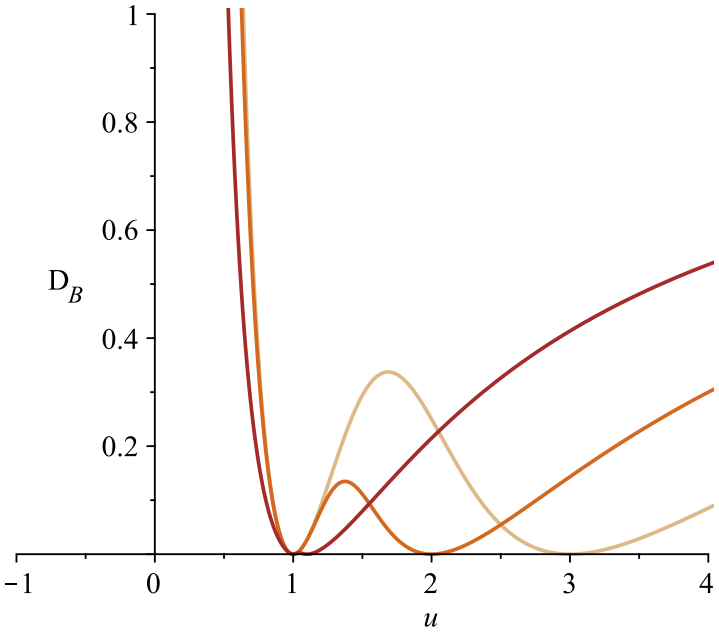

Here, $\varepsilon = 2$ is represented byt the light brown/gold curve, $\varepsilon = 1$ by the orange curve, and $\varepsilon = .1$ by the dark red/brown curve.

Below we provide two dispersion relation plots in the $n_B = 2$ case to illustrate this surprising behavior and to contrast the instability node behavior in the one-stream case ($\mathring{v}_1 = \mathring{v}_2$) from the two-streams merging case ($\mathring{v}_2 = \mathring{v}_1 + \varepsilon$). Both plots assume $\beta_1 = .3, \beta_2 = .7$, and $\mathring{v}_1 = 1$ while $\mathring{v}_2$ varies. As our analysis suggests, both ω and $\Re(k)$ tend to infinity:

In short, the disappearance of the point u_c in the one-stream case can be viewed as a collapse of power in the two-stream characteristic equation eq. (4.13). For this reason, to study the solutions u to eq. (4.13) as the two streams merge requires advanced analytic function theory involving the study of algebraic functions at exceptional points, as seen in [17], for example.

Thankfully, there is a more elementary approach that can be taken by making use of the theory of Puiseux series, which is the main subject of our studies here. To pursue this line of argument, however, we first need a way to represent solutions u to $D_B(u) = 1/\omega^2$ that

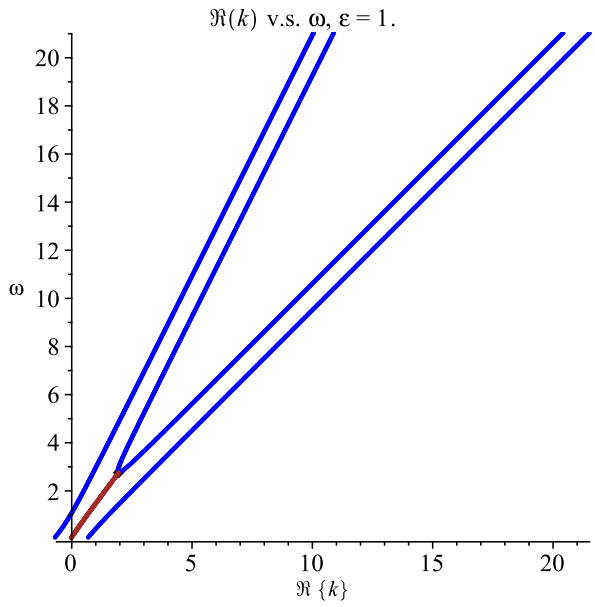

Figure 4.3: $\mathring{v}_1 = 1, \mathring{v}_2 = 2$.

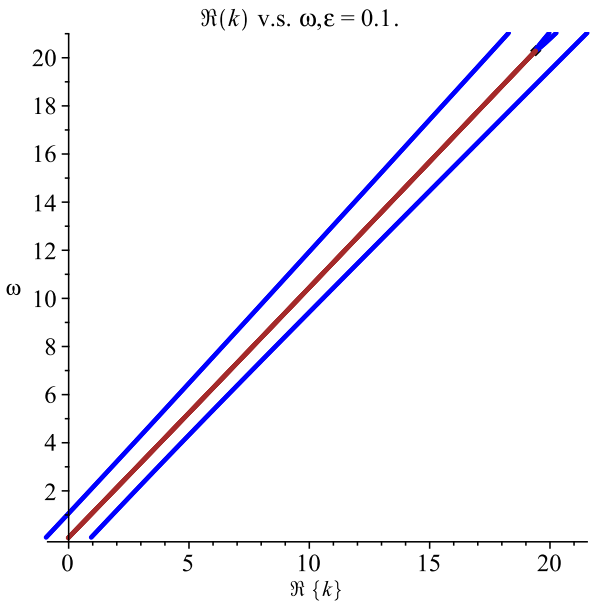

Figure 4.4: $\mathring{v}_1 = 1, \mathring{v}_2 = 1.1$.

avoids the singularity behavior ($\omega_c \to \infty$) when $\mathring{v}_2$ and $\mathring{v}_1$ are close. For this reason, we introduce a change of variables.

4.4 Change of variables and a new characteristic equation

As prompted by our previous discussion, instead of studying solutions we introduce a linear change of variables from u to s as follows:

$$u = \frac{1}{\left(\frac{1}{\mathring{v}_1} - \frac{1}{\mathring{v}_2}\right) s + \frac{1}{\mathring{v}_2}}, \quad s = \frac{\mathring{v}_1 \mathring{v}_2}{\mathring{v}_2 - \mathring{v}_1} \frac{1}{u} - \frac{\mathring{v}_1}{\mathring{v}_2 - \mathring{v}_1}. \tag{4.26}$$

Here, we only consider $u \in (\mathring{v}_1, \mathring{v}_2)$ and hence, $s \in (0, 1)$. Since we are interested in the behavior of solutions near the branching point at which solutions transition from complex to real, i.e. near the critical point u_c of D_B and $u_c \in (\mathring{v}_1, \mathring{v}_2)$, the bounds on s are appropriate.

Consequently, the critical point s_c of T_B (given below) is in $(0, 1)$.

This recasts the function D_B into T_B:

$$T_B(s) = \frac{b}{s^2} + \frac{1}{(1-s)^2} \tag{4.27}$$

where the new parameters b and B are defined as follows:

$$B = \frac{\beta_1 \mathring{v}_2^2}{(\mathring{v}_2 - \mathring{v}_1)^2}, \quad b = \frac{\beta_2 \mathring{v}_1^2}{\beta_1 \mathring{v}_2^2}. \tag{4.28}$$

Consequently, the new characteristic equation in terms of s is given by:

$$T_B(s) = \frac{b}{s^2} + \frac{1}{(1-s)^2} = \omega'^2, \tag{4.29}$$

where $\omega' = \omega/\sqrt{B}$.

Some properties of the function T_B are given in the following theorem.

Theorem 4.4.1. Define T_B as in eq. (4.27). Then,

1. T_B has two real poles at $s = 0, 1$,
2. for $s \in \mathbb{R}$, $T_B(s) > 0$, and
3. for $s \in \mathbb{C}$ and $\omega' > 0$, eq. (4.29) has four solutions.

Proof. We observe immediately from eq. (4.27) that function T_B has poles at $s = 0, 1$. When $s \in \mathbb{R}$, $T_B(s)$ has no zeros since both b/s^2 and $1/(1-s)^2$ are positive. Thus $T_B(s) > 0$ for all real s. Rationalizing $T_B(s)$, we obtain:

$$T_B(s) = \frac{b(1-s)^2 + s^2}{s^2(1-s)^2}. \tag{4.30}$$

Thus solutions s to $T_B(s) - \omega'^2$ are solutions to the quartic polynomial:

$$-\omega'^2 s^4 + 2\omega'^2 s^3 + (b + 1 - \omega'^2)s^2 - 2bs + b. \tag{4.31}$$

Since $\omega' > 0$, this polynomial is always degree 4, and hence we always obtain four solutions to eq. (4.29). □

From the previous argument, depending on the value chosen for ω', solutions to the T_B equation may consist of four real solutions or two real solutions and one pair of complex solutions.

For $s \in \mathbb{R}$, the graph of $T_B(s)$ is given below (here, $\beta_1 = .3, \beta_2 = .7, \mathring{v}_1 = 1, \mathring{v}_2 = 3$ and $b = 7/27$):

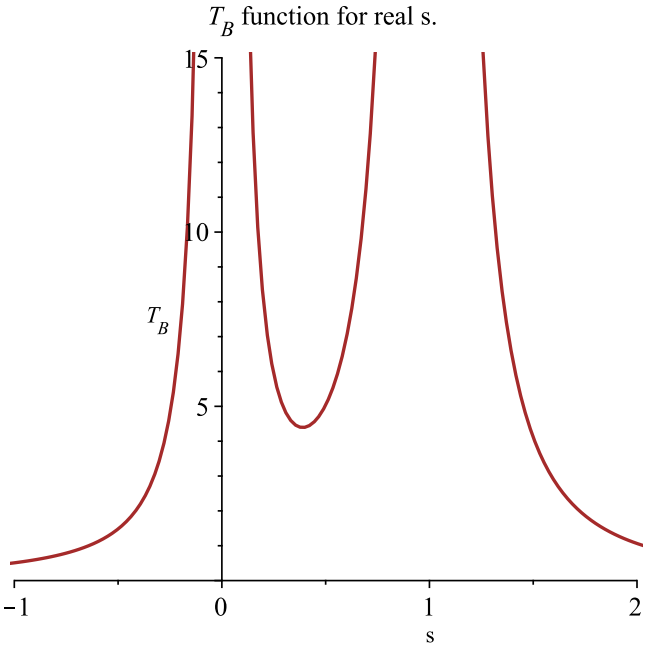

From the graph, we see that the critical point $s_c \in (0, 1)$ provides the frequency at which solutions transition from non-real to real: $\omega'_c = \sqrt{T_B(s_c)}$. In particular, if $\omega' \in [0, \omega'_c]$ then solutions $s \in (0, 1)$ to $T_B(s)$ will consist of one pair of complex conjugate solutions. If

$\omega' \in [\omega'_c, \infty)$ then the solutions will be real.

Theorem 4.4.2. For $s \in (0,1)$, $T_B(s)$ has one real critical point $s_c = \sqrt[3]{b}/(1+\sqrt[3]{b})$ with corresponding frequency $\omega_c'^2 = (b^{1/3}+1)^3$.

Proof. We can explicitly compute the real critical point s_c of $T_B(s)$ by differentiating $T_B(s)$ and equating it with 0:

$$T'_B(s) = \frac{2}{(1-s)^3} - \frac{2b}{s^3}, \tag{4.32}$$

so $T'_B(s) = 0$ when

$$\frac{2}{(1-s)^3} = \frac{2b}{s^3}, \tag{4.33}$$

and hence

$$\sqrt[3]{b} = \frac{s}{1-s}. \tag{4.34}$$

Finally, solving for s, we have that the real critical point, s_c of T_B occurs when

$$s_c = \frac{\sqrt[3]{b}}{1+\sqrt[3]{b}}. \tag{4.35}$$

Evaluating T_B at $s = s_c$ and taking the square root of the result, we see that the corresponding ω' value, ω_c is precisely:

$$\omega'_c = \sqrt{(b^{1/3}+1)^3}. \tag{4.36}$$

□

Our goal now is to express the solutions s to $T_B(s) = \omega'^2$ in terms of b and ω', which we do

in the following section.

4.5 Series representation of solutions near the critical point

Our main result is that solutions s to the characteristic equation $T_B(s) = \omega'^2$ near the transition point $(s_c, \omega_c'^2)$ can be expressed as a convergent Puiseux series [27] which we explicitly compute. More precisely:

Theorem 4.5.1. Let s_c be the real critical point of eq. (4.27) in $(0,1)$ so that $T_B'(s_c) = 0$ and $T_B(s_c) = \omega_c'^2$. Then, there are $\delta > 0$ and $\eta > 0$ so that if $\omega' \in (\omega_c' - \eta, \omega_c' + \eta) \backslash \{\omega_c'\}$, then

1. there are exactly two distinct solutions $s \in \mathbb{C}$ to $T_B(s) = \omega'^2$ with $s \in D_\delta(s_c)$, and
2. for both solutions s_+ and s_-, there is a Puiseux series representation centered at ω_c' with radius of convergence at least η, i.e.:

$$s_\pm(\omega') = s_c + \sum_{n=1}^{\infty} A_n (\pm\sqrt{\omega' - \omega_c'})^n$$

where the A_n coefficients are algebraic expressions of the parameter b.

The first few b_n coefficients are computed explicitly and given in eq. (4.44).

Proof. The function T_B is analytic everywhere except for $s = 0, 1$ and bounded away from 0 (as we saw in theorem 4.4.1). Thus, $\sqrt{T_B(s)}$ is analytic in some disk $D_\delta(s_c)$, centered at s_c with radius $\delta > 0$. We claim that $\sqrt{T_B}$ satisfies the hypotheses of theorem A.2.3.

We note that $T_B(s_c) = {\omega'_c}^2 = (b^{1/3}+1)^3$ and $T'_B(s_c) = 0$. Moreover, $T''_B(s_c) = 6({\omega'_c})^{10/3}b^{-1/3} \neq 0$, so s_c is a critical point of T_B of order two. Then we can show that s_c is also a critical point of order two for $\sqrt{T_B(s)}$, since:

$$(\sqrt{T_B(s)})' = \frac{T'_B(s)}{2\sqrt{T'_B(s)}}. \tag{4.37}$$

Evaluating at $s = s_c$ yields 0, so s_c is a critical point of $\sqrt{T_B}$. Computing the second derivative, we have:

$$(\sqrt{T_B(s)})'' = \frac{-T'_B(s)}{4(T_B(s))^{3/2}} + \frac{T''_B(s)}{2\sqrt{T_B(s)}}. \tag{4.38}$$

Evaluating at s_c, we see that $T''_B(s_c) \neq 0$. Thus, according to theorem A.2.3, we can express solutions $s = s(\omega')$ to $\sqrt{T_B(s)} = \omega'$ as a Puiseux series which converges in the punctured disk $D_\eta(\omega'_c)\backslash\{\omega'_c\}$ where $\eta > 0$.

We can find the series expansion for $\sqrt{T_B(s)}$ by first computing the Taylor series of $T_B(s)$ centered at s_c:

$$\omega'^2 = T_B(s) = \sum_{n=0}^{\infty} \frac{T_B^{(n)}(s_c)}{n!}(\Delta s)^n = {\omega'_c}^2 + \sum_{n\geq 2} \frac{T_B^{(n)}(s_c)}{n!}(\Delta s)^n, \tag{4.39}$$

where $\Delta s = s - s_c$. Taking the square root, we obtain

$$\omega' = \sqrt{T_B(s)} = \omega'_c + \sum_{n\geq 2} a_n(\Delta s)^n, \tag{4.40}$$

where the a_n are given by theorem A.2.2. Now, if $\Delta\omega' = \omega' - \omega'_c$, we have:

$$\Delta\omega' = \sum_{n\geq 2} a_n(\Delta s)^n = (a_2\Delta s^2)\left(1 + \sum_{n\geq 3} \frac{a_n}{b_2}\Delta s^{n-2}\right). \tag{4.41}$$

Taking the square root, again according to theorem A.2.2, we have for some coefficients c_n:

$$\pm\sqrt{\Delta\omega'} = (\sqrt{b_2}\Delta s)\left(1+\sum_{n\geq 3}\frac{b_n}{b_2}(\Delta s)^{n-2}\right)^{1/2} = \sum_{n\geq 1} c_n \Delta s^n. \tag{4.42}$$

Now, we can invert (revert) the series $\pm\sqrt{\Delta\omega'} = \sum_{n\geq 1} c_n \Delta s^n$ according to theorem A.2.1:

$$\Delta s = \frac{1}{c_1}(\pm\sqrt{\Delta\omega'}) - \frac{c_2}{c_1^3}(\pm\sqrt{\Delta\omega'})^2 + \frac{-c_1c_3+2c_2^2}{c_1^5}(\pm\sqrt{\Delta\omega'})^3 + O((\pm\sqrt{\Delta\omega'})^4). \tag{4.43}$$

Computing the coefficients explicitly, we have:

$$\begin{aligned} s_\pm =& s_c \pm \frac{1}{3}\frac{\sqrt{6}\sqrt[6]{b}}{\left(\sqrt[3]{b}+1\right)^{7/4}}\sqrt{\Delta\omega'} - \frac{4}{9}\frac{\left(\sqrt[3]{b}-1\right)}{\left(\sqrt[3]{b}+1\right)^{5/2}}\Delta\omega' \\ &\pm \frac{\sqrt{6}(20b^{2/3}-73b^{1/3}+20)}{324b^{1/6}(\sqrt[3]{b}+1)^{13/4}}\sqrt{\Delta\omega'}^3 + O((\pm\sqrt{\Delta\omega'})^4). \end{aligned} \tag{4.44}$$

□

The series representation eq. (4.44) can be used to approximate solutions to $T_B(s) = \omega'^2$ when s and s_c are close as accurately as desired. When $\Delta\omega' < 0$, i.e. $\omega' < \omega'_c$ we obtain two complex conjugate solutions, and when $\Delta\omega' > 0$ we have two real solutions as expected. In particular, the terms corresponding to odd powers of n, $(\pm\sqrt{\Delta\omega'})^n$, give the imaginary part of s whenever $s \notin \mathbb{R}$.

Reverting back to the original parameters $\mathring{v}_1, \mathring{v}_2, \hat{\beta}_1, \hat{\beta}_2$ (see eq. (4.28)), we can rewrite the Puiseux expansion eq. (4.44) in terms of the original variables u and ω according to the change of variables in eq. (4.26). The explicit representation of u as a function of ω is quite messy, so we write here only the first order approximation $s \approx s_c + a_1(\pm\sqrt{\Delta\omega'})$:

$$
\begin{aligned}
u &\approx \frac{\mathring{v}_1\mathring{v}_2}{(\mathring{v}_2-\mathring{v}_1)(s_c \pm \frac{1}{3}\frac{\sqrt{6}\sqrt[6]{b}}{(\sqrt[3]{b}+1)^{7/4}}\sqrt{\Delta\omega'}) + \mathring{v}_1} \\
&= \frac{\mathring{v}_1\mathring{v}_2}{(\mathring{v}_2-\mathring{v}_1)\left(\frac{\sqrt[3]{\frac{\beta_2\mathring{v}_1^2}{\beta_1\mathring{v}_2^2}}}{\sqrt[3]{\frac{\beta_2\mathring{v}_1^2}{\beta_1\mathring{v}_2^2}}+1} \pm \frac{\sqrt{6}}{3}\frac{\sqrt[6]{\frac{\beta_2\mathring{v}_1^2}{\beta_1\mathring{v}_2^2}}}{\left(\sqrt[3]{\frac{\beta_2\mathring{v}_1^2}{\beta_1\mathring{v}_2^2}}+1\right)^{7/4}}\sqrt{\frac{(\mathring{v}_2-\mathring{v}_1)\omega}{\sqrt{\beta_1}\mathring{v}_2} - \left(\sqrt[3]{\frac{\beta_2\mathring{v}_1^2}{\beta_1\mathring{v}_2^2}}+1\right)^{3/2}}\right) + \mathring{v}_1}
\end{aligned}
\tag{4.45}
$$

4.5.1 Accuracy of the series representation

To see the accuracy of the series approximation given by eq. (4.44), we provide two plots: ω' vs. $\Re(s)$ and ω' vs. $\Im(s)$ for the following data:

β_1	β_2	$\mathring{v}_1$	$\mathring{v}_2$	b
.3	.7	1	3	$\frac{7}{27}$

Here, b is computed according to eq. (4.28) For varying ω' in the interval $(1,3)$, we solve the characteristic equation $T_B(s) = \omega'^2$ for s first, explicitly and second, according to the series approximation given by eq. (4.44). Using the given data in the table and according to eq. (4.35) and eq. (4.36), we can easily compute:

$$
\begin{aligned}
s_c &= \frac{b^{1/3}}{b^{1/3}+1} \approx 0.3894 \text{ and} \\
\omega'_c &= (b^{1/3}+1)^{3/2} \approx 2.0957.
\end{aligned}
\tag{4.46}
$$

In both plots, the red curve is obtained from the explicit computation of the solutions s to $T_B(s) = \omega'^2$, while the blue curve is obtained from the series approximation given in eq. (4.44).

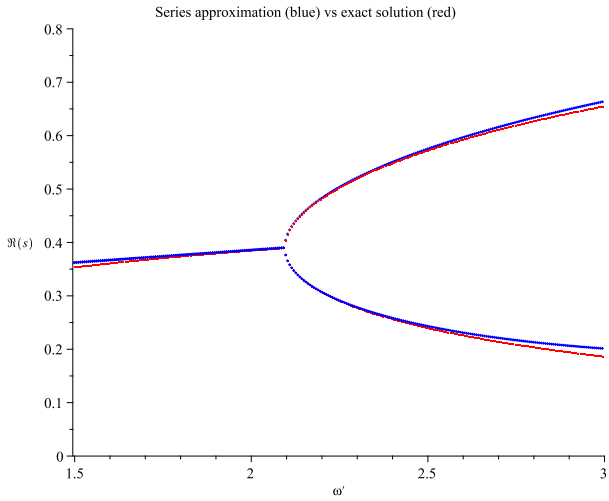

Figure 4.5: ω' vs $\Re(s)$

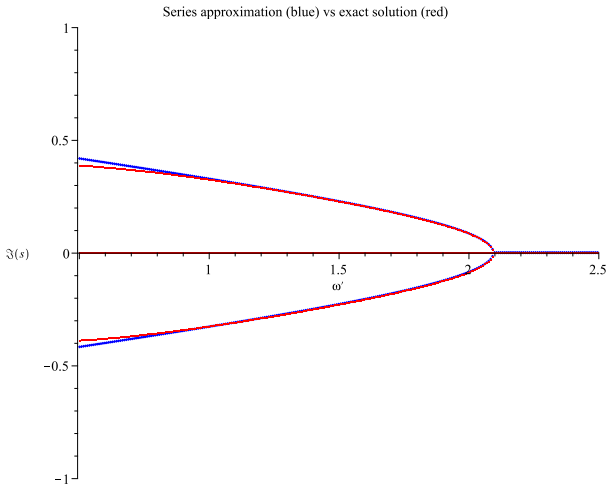

Figure 4.6: ω' vs $\Im(s)$

4.6 The imaginary part of non-real solutions

In this section, we show that as suggested by Figure 4.6, if s is a non-real solution to $T_B(s) = \omega'^2$, then $\Im(s)$ is bounded, and, using the series representation eq. (4.44), we see that as $\omega' \to \omega'_c$, $\Im(s) \to 0$. More precisely:

Theorem 4.6.1. Let $\omega' \in [0, \omega'_c]$. If s is a non-real solution to $T_B(s) = \omega'^2$, then $\Im(s)$ is bounded. Moreover

$$\lim_{\omega' \to \omega'_c{}^-} \Im(s) = 0. \tag{4.47}$$

Proof. When $\omega' = 0$, we can solve $T_B(s) = \omega'^2$ explicitly. If

$$\frac{b}{s^2} + \frac{1}{(1-s)^2} = 0, \tag{4.48}$$

then we obtain two complex conjugate solutions

$$s_\pm = \frac{b \pm i\sqrt{b}}{b+1}. \tag{4.49}$$

We will denote the solution $s_\pm$ with positive imaginary part by s_0 and note that the same argument holds if we choose s_0 with negative imaginary part.

To see that $\Im(s)$ is bounded near $\omega' = 0$, we apply the Implicit Function Theorem for Banach spaces (see theorem A.3.1).

Writing $T_B(s) = \omega'^2$ as

$$f(\omega', s) = \frac{b}{s^2} + \frac{1}{(1-s)^2} - \omega'^2, \tag{4.50}$$

we have $f : \mathbb{R} \times \mathbb{C} \to \mathbb{C}$.

Previously, we only considered $\omega' \geq 0$, when studying solutions s to $T_B(s) = \omega'^2$; however, by symmetry, we can also consider $\omega' < 0$, since $T_B(s) = \omega'^2 = (-\omega')^2$. Consider a small open interval I around $\omega' = 0$ and any open neighborhood U of s_0 so that $0, 1 \notin U$ (for example, we can take U to be the upper half plane in $\mathbb{C}$). Then f is Frechet differentiable in $I \times U$ and $f(0, s_0) = 0$.

Then,

$$f_s(\omega', s) = \frac{-2b}{s^3} + \frac{2}{(1-s)^3}. \tag{4.51}$$

Thus, we see that $f_s = 0$ at $(s_c, \omega_c'^2)$ where $s_c = \sqrt[3]{b}/(1 + \sqrt[3]{b})$. In particular, this means that $f_s(0, s_0) \neq 0$, i.e. f_s is invertible.

Thus, by the Implicit Function Theorem, there are $r, \rho > 0$ so that if $\omega' \in (-r, r)$, then there is a unique $s(\omega') \in B(s_0, \rho)$ satisfying

$$f(\omega', s(\omega')) = 0 \tag{4.52}$$

and $s(\omega')$ is continuous. Thus $s(\omega')$ is bounded on $[0, r]$.

For $\omega' \in (r, {\omega'}_c)$, solutions s to

$$\frac{b}{s^2} + \frac{1}{(1-s)^2} = {\omega'}^2 \tag{4.53}$$

must have bounded imaginary part. Otherwise, if $\Im(s)$ is unbounded, then $||s||$ is unbounded too. Thus,

$$\lim_{|s|\to\infty} \left|\left| \frac{b}{s^2} + \frac{1}{(1-s)^2} \right|\right| = 0, \tag{4.54}$$

i.e. the left-hand side of eq. (4.53) tends to 0 in norm so that the right-hand side, ${\omega'}^2$ also tends to 0, but $\omega' > r > 0$.

Thus, $\Im(s)$ is bounded for all $\omega' \in [0, {\omega'}_c]$.

Now, let us consider solutions s near the transition point s_c, and recall that $s_c = \frac{\sqrt[3]{b}}{1+\sqrt[3]{b}}$, so $\Im(s_c) = 0$. we have seen with the series representation given in eq. (4.44) that as $\omega' \to {\omega'}_c$, $s \to s_c$. This also implies that $\Im(s) \to 0$, since $\Im(s)$ is given precisely by the odd terms of the series (again, because $\omega' < {\omega'}_c$). In particular,

$$\Im(s) = \sum_{k=0}^{\infty} a_k (\sqrt{{\omega'}^2 - {\omega'}_c^2})^{2k+1}, \tag{4.55}$$

which clearly tends to 0 as $\omega' \to {\omega'}_c$. □

Corollary 4.6.1. $\omega' = 0$ is a local extreme value of the function $\Im(s)(\omega')$ with value $\Im(s)(0) = \frac{\sqrt{b}}{b+1}$.

Proof. Using the same notation from the theorem,

$$f(\omega', s) = \frac{b}{s^2} + \frac{1}{(1-s)^2} - {\omega'}^2 \tag{4.56}$$

is also differentiable with respect to ω' and $f_{\omega'}(s, \omega') = -2\omega'$. Then, according to the Implicit Function Theorem, we have:

$$s'(\omega') = -\frac{-2\omega'}{\frac{-2b}{s^3} + \frac{2}{(1-s)^3}} = \frac{-\omega'}{\frac{-b}{s^3} + \frac{1}{(1-s)^3}} \tag{4.57}$$

when (ω', s_0) is near $(0, s_0)$. Using this formula, we have $s'(0) = 0$, and so $\Im(s)'(0) = 0$. Since $\omega' = 0$ when $s = s_0$, this implies that $\Im(s)(0) = \Im(s_0) = \Im((b + i\sqrt{b})/(b+1)) = \sqrt{b}/(b+1)$.

□

Chapter 5

Solutions to the characteristic equation: merging streams

One of our goals is top use the series representation obtained in the previous chapter to study the behavior of the solutions s to $T_B(s) = \omega'^2$ when the two real poles $\mathring{v}_1, \mathring{v}_2$ are close.

For $\beta_1 = .3, \beta_2 = .7$, we consider $\mathring{v}_1 = 1$ and $\mathring{v}_2 = \mathring{v}_1 + \varepsilon$. The graph below shows three $T_{B,\varepsilon}(s)$ graphs for real s and varying ε: $\varepsilon = 1$, (red curve), $\varepsilon = .5$ (blue curve), and $\varepsilon = 0$ (green curve). Note that the critical point s_c of $T_{B,\varepsilon}(s)$ is increasing as $\varepsilon \to 0$:

One benefit of the change of variables from u to s and resulting characteristic equation T_B is that the frequency ω'_c is bounded as $\varepsilon \to 0$, unlike the behavior of ω_c which we saw in theorem 4.3.1. Thus the Puiseux series obtained in the previous chapter eq. (4.44) can be used to study solutions $s = s(\omega')$ and their dependence on ε.

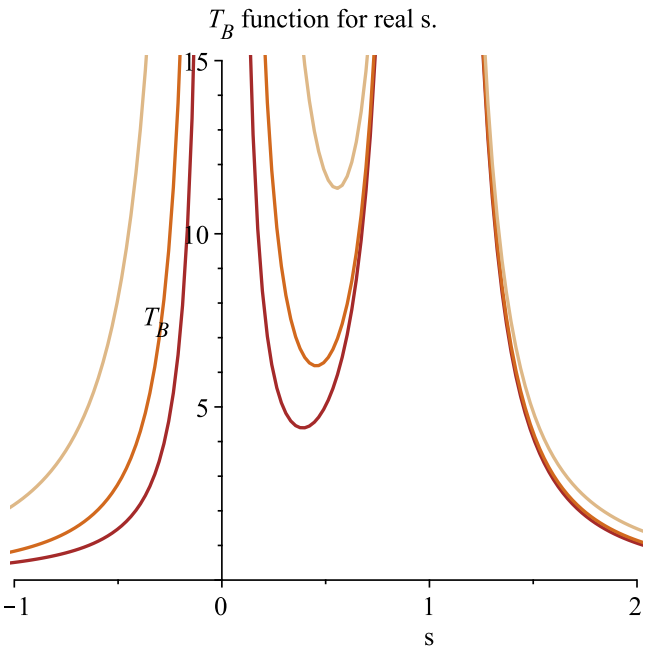

Figure 5.1: Here, $\varepsilon = 2$ is represented by the dark brown/red curve, $\varepsilon = 1$ by the orange curve, and $\varepsilon = .1$ by the light brown/gold curve.

5.1 Behavior of the critical point and solutions to the characteristic equation for merging streams

In this section we study the behavior of the critical point s_c, its corresponding ${\omega'}_c$ value, and solutions s to $T_B(s) = {\omega'}^2$ as $\mathring{v}_2 \to \mathring{v}_1$. To do so, we define the dependence on ε for the parameter b and the function T_B.

In what follows, the merging of streams is modeled by defining $\mathring{v}_2 = \mathring{v}_1 + \varepsilon$ and small $\varepsilon > 0$. Note that since

$$b = \frac{\beta_2 \mathring{v}_1^2}{\beta_1 \mathring{v}_2^2}, \tag{5.1}$$

b now depends on ε:

$$b_\varepsilon = \frac{\beta_2 \mathring{v}_1^2}{\beta_1(\mathring{v}_1 + \varepsilon)^2}. \tag{5.2}$$

The function $T_{B,\varepsilon}(s)$ is defined as:

$$T_{B,\varepsilon}(s) = \frac{b_\varepsilon}{s^2} + \frac{1}{(s-1)^2}. \tag{5.3}$$

Making use of our formulas eq. (4.35), eq. (4.36) we have that the critical point $s_{c,\varepsilon}$ and corresponding frequency value ${\omega'}_{c,\varepsilon}$ are given by:

$$s_{c,\varepsilon} = \frac{\sqrt[3]{b_\varepsilon}}{1 + \sqrt[3]{b_\varepsilon}} \text{ and} \tag{5.4}$$

$${\omega'}_{c,\varepsilon} = \sqrt{(b_\varepsilon^{1/3} + 1)^3}. \tag{5.5}$$

From these definitions, we have some simple consequences of the behavior of $b_\varepsilon, s_{c,\varepsilon}, {\omega'}_{c,\varepsilon}$ as $\varepsilon \to 0$:

Theorem 5.1.1. Let $b_\varepsilon, s_{c,\varepsilon}$, and ${\omega'}_{c,\varepsilon}$ be defined as in eq. (5.2) and eqs. (5.4) to (5.5). Then, as $\varepsilon \to 0$:

1. b_ε, $s_{c,\varepsilon}$ and ${\omega'}_{c,\varepsilon}$ are all increasing,
2. $\lim_{\varepsilon \to 0} b_\varepsilon = \bar{b}$ where $\bar{b} = \frac{\beta_2}{\beta_1}$, and consequently,
3. $\lim_{\varepsilon \to 0} s_{c,\varepsilon} = \frac{\bar{b}^{1/3}}{1+\bar{b}^{1/3}}$, and $\lim_{\varepsilon \to 0} {\omega'}_{c,\varepsilon} = \sqrt{\left(\bar{b}^{1/3} + 1\right)^3}$.

Proof. We note that

$$\lim_{\varepsilon\to 0} b_\varepsilon = \lim_{\varepsilon\to 0} \frac{\beta_2 \mathring{v}_1^2}{\beta_1(\mathring{v}_1+\varepsilon)^2} = \frac{\beta_2}{\beta_1}. \tag{5.6}$$

We denote $\bar{b} = \beta_2/\beta_1$. Moreover, b_ε is monotonically increasing as $\varepsilon \to 0$, since β_1, β_2 are fixed and $\mathring{v}_1^2/(\mathring{v}_1+\varepsilon)^2$ is increasing. We also see that bounded

$$0 < b_\varepsilon \leq \bar{b}. \tag{5.7}$$

It is also easy to see that for $x \in \mathbb{R}$, $f(x) = \frac{\sqrt[3]{x}}{1+\sqrt[3]{x}}$ is an increasing function. From this we may conclude that $s_{c,\varepsilon}$ is increasing as $\varepsilon \to 0$ and bounded. In particular,

$$\lim_{\varepsilon\to 0} s_{c,\varepsilon} = \lim_{\varepsilon\to 0} \frac{\sqrt[3]{b_\varepsilon}}{1+\sqrt[3]{b_\varepsilon}} = \frac{\sqrt[3]{\bar{b}}}{1+\sqrt[3]{\bar{b}}} = \frac{\sqrt[3]{\beta_2/\beta_1}}{1+\sqrt[3]{\beta_2/\beta_1}} \tag{5.8}$$

As for the critical value of ω', it too is bounded and monotonically increasing. For $\varepsilon > 0$, we have:

$$\begin{aligned} \lim_{\varepsilon\to 0} {\omega'}_{c,\varepsilon} &= \lim_{\varepsilon\to 0} \sqrt{(1+\sqrt[3]{b_\varepsilon})^3} \\ &= \sqrt{(1+\sqrt[3]{\bar{b}})^3} \\ &= \sqrt{(1+\sqrt[3]{\beta_2/\beta_1})^3} \end{aligned} \tag{5.9}$$

Moreover, $1 \leq {\omega'}_{c,\varepsilon} \leq {\omega'}_c$. □

5.2 Merging streams: solutions near the critical point

In this section for fixed ω, we analyze solutions s to

$$T_{B,\varepsilon} = {\omega'_\varepsilon}^2 \tag{5.10}$$

near the critical point $s_{c,\varepsilon}$ as the two streams merge ($\mathring{v}_2 = \mathring{v}_1 + \varepsilon, \varepsilon \to 0$). Note that:

$$\omega'_\varepsilon = \frac{\omega}{\sqrt{B_\varepsilon}} = \frac{\omega}{\sqrt{\frac{\beta_1(\mathring{v}_1+\varepsilon)^2}{\varepsilon^2}}} = \frac{\varepsilon\omega}{\sqrt{\beta_1}(\mathring{v}_1+\varepsilon)}. \tag{5.11}$$

Making use of our series representation given in eq. (4.44) for solutions s to $T_B(s) = \omega'^2$ near s_c, we analyze the behavior of these solutions when the two streams merge. The resulting dependence on ε is given by:

$$\begin{aligned} s_\varepsilon \approx & s_{c,\varepsilon} \pm \frac{1}{3}\frac{\sqrt{6}\sqrt[6]{b_\varepsilon}}{\left(\sqrt[3]{b_\varepsilon}+1\right)^{7/4}}\sqrt{\omega'_\varepsilon - \omega'_{c,\varepsilon}} - \frac{4}{9}\frac{\left(\sqrt[3]{b_\varepsilon}-1\right)}{\left(\sqrt[3]{b_\varepsilon}+1\right)^{5/2}}(\omega'_\varepsilon - \omega'_{c,\varepsilon}) \\ & \pm \frac{\sqrt{6}({b_\varepsilon}^{2/3} - 73{b_\varepsilon}^{1/3} + 20)}{324{b_\varepsilon}^{1/6}(\sqrt[3]{b_\varepsilon}+1)^{13/4}}\sqrt{\omega'\varepsilon - \omega'_{c,\varepsilon}}^3 + O((\pm\sqrt{\omega'_\varepsilon - \omega'_{c,\varepsilon}})^4). \end{aligned} \tag{5.12}$$

Making the substitutions given by eq. (5.2), eq. (5.4), eq. (5.5), and eq. (5.11), we have:

$$\begin{aligned} s_\varepsilon \approx & \frac{\sqrt[3]{b_\varepsilon}}{1+\sqrt[3]{b_\varepsilon}} \pm \frac{1}{3}\frac{\sqrt{6}\sqrt[6]{b_\varepsilon}}{\left(\sqrt[3]{b_\varepsilon}+1\right)^{7/4}}\sqrt{\frac{\varepsilon\omega}{\sqrt{\beta_1}(\mathring{v}_1+\varepsilon)} - \sqrt{({b_\varepsilon}^{1/3}+1)^3}} \\ & - \frac{4}{9}\frac{\left(\sqrt[3]{b_\varepsilon}-1\right)}{\left(\sqrt[3]{b_\varepsilon}+1\right)^{5/2}}\left(\frac{\varepsilon\omega}{\sqrt{\beta_1}(\mathring{v}_1+\varepsilon)} - \sqrt{({b_\varepsilon}^{1/3}+1)^3}\right) \\ & \pm \frac{\sqrt{6}(20{b_\varepsilon}^{2/3} - 73{b_\varepsilon}^{1/3}+20)}{324{b_\varepsilon}^{1/6}(\sqrt[3]{b_\varepsilon}+1)^{13/4}}\sqrt{\frac{\varepsilon\omega}{\sqrt{\beta_1}(\mathring{v}_1+\varepsilon)} - \sqrt{({b_\varepsilon}^{1/3}+1)^3}}^3 \\ & + O\left(\left(\pm\sqrt{\frac{\varepsilon\omega}{\sqrt{\beta_1}(\mathring{v}_1+\varepsilon)} - \sqrt{({b_\varepsilon}^{1/3}+1)^3}}\right)^4\right). \end{aligned} \tag{5.13}$$

Then, for fixed ω, as $\varepsilon \to 0$, we have:

$$\begin{aligned} s \approx & \frac{\sqrt[3]{\beta_2/\beta_1}}{1+\sqrt[3]{\beta_2/\beta_2}} \pm \frac{1}{3}\frac{\sqrt{6}\sqrt[6]{\beta_2/\beta_1}}{\left(\sqrt[3]{\beta_2/\beta_1}+1\right)^{7/4}}\sqrt{-\sqrt{\left(1+\sqrt[3]{\beta_2/\beta_1}\right)^3}} \\ & - \frac{4}{9}\frac{\left(\sqrt[3]{\beta_2/\beta_1}-1\right)}{\left(\sqrt[3]{\beta_2/\beta_1}+1\right)^{5/2}}\left(-\sqrt{(1+\sqrt[3]{\beta_2/\beta_1})^3}\right) \\ & \pm \frac{\sqrt{6}(20\sqrt[3]{\beta_2/\beta_1}^2 - 73\sqrt[3]{\beta_2/\beta_1}+20)}{324\sqrt[3]{\beta_2/\beta_1}^{1/2}(\sqrt[3]{\beta_2/\beta_1}+1)^{13/4}}\left(\sqrt{-\sqrt{(1+\sqrt[3]{\beta_2/\beta_1})^3}}\right)^3 \\ & + O\left(\left(\pm\sqrt{-\sqrt{(1+\sqrt[3]{\beta_2/\beta_1})^3}}\right)^4\right). \end{aligned} \tag{5.14}$$

In this case, we see that as expected, if ω is fixed and $\varepsilon \to 0$, the representation gives solutions s which are always non-real.

Appendices

A.1 Rouche's Theorem

We paraphrase here the formulation of Rouche's theorem as described in [17].

Theorem A.1.1 (Rouche's Theorem)**.** Let γ be a simple, closed rectifiable (Jordan curve). Suppose that $F(z)$ and $G(z)$ are meromorphic functions inside and on a vicinity of γ, and $G(z)$ does not have zeros or poles on γ. Suppose also that

$$|F(z) - G(z)| < |G(z)|,\ z \in \gamma.$$

Then if Z_F and P_F stand respectively for the number of zeros and poles of $F(z)$ inside γ, the difference between the number of zeros and the number of poles is the same for both functions $F(z)$ and $G(z)$, that is $Z_F - P_F = Z_G - P_G$.

A.2 Theorems for series reversion and square roots

In chapter 4, we express solutions to eq. (4.29) as a Puiseux series using the reversion formula given by Lagrange's series as well as the square root of a series formula found in [5], [1]. We formulate those theorems in this section.

Theorem A.2.1 (Lagrange's series)**.** Let $F(z)$ be an analytic function of z in a vicinity of $z = z_0$ with the Taylor expansion

$$F(z) = \sum_{n\geq 1} a_n (z - z_0)^n, a_n = \frac{\partial^n F(z_0)}{n!}, F(z_0) = 0, F'(z_0) = a_1 \neq 0. \tag{15}$$

Then there is a sufficiently small vicinity of $z = z_0$ where the function $F(z)$ has inverse $G(z)$, that is $G(F(z)) = z - z_0$, satisfying the Lagrange series expansion:

$$G(w) = \sum_{n\geq 1} g_n w^n, g_n = \frac{1}{n!} \frac{d^{n-1}}{dz^{n-1}} \left(\frac{z}{F(z)}\right)^n \Big|_{z=z_0}. \tag{16}$$

The first five terms of the expansion above are given by:

$$\begin{aligned} G(w) = &\frac{1}{a_1} w - \frac{a_2}{a_1^3} w^2 + \frac{-a_1 a_3 + 2a_2^2}{a_1^5} w^3 + \frac{-a_1^2 a_4 + 5a_1 a_2 a_3 - 5a_2^3}{a_1^7} w^4 \\ &+ \frac{-a_5 a_1^3 + 6a_2 a_4 a_1^2 + 3a_3^2 a_1^2 - 21 a_2^2 a_3 a_1 + 14 a_2^4}{a_1^9} w^5 + O(w^6). \end{aligned}$$

Theorem A.2.2. Consider the formal power series

$$\sum_{n\geq 0} a_n z^n. \tag{17}$$

Then square root of this series can be computed according to the following formula, provided $a_0 \neq 0$:

$$\sqrt{\sum_{n\geq 0} a_n z^n} = \sqrt{a_0}\left[1 + \frac{a_1}{2a_0}z + \left(-\frac{a_1^2}{8a_0^2} + \frac{a_2}{2a_0}\right)z^2 + \left(\frac{a_1^3}{16a_0^3} - \frac{a_1 a_2}{4a_0^2} + \frac{a_3}{2a_0}\right)z^3 \right. \tag{18}$$

$$\left. = + \left(-\frac{5a_1^4}{128a_0^4} + \frac{3a_1^2 a_2}{16a_0^3} - \frac{a_1 a_3}{4a_0^2} - \frac{a_2^2}{8a_0^2} + \frac{a_4}{2a_0}\right)z^4 + O(z^5)\right]. \tag{19}$$

In the special case when $a_0 = 1$, the above equation simplifies to:

$$\sqrt{1 + \sum_{n\geq 1} a_n z^n} = 1 + \frac{a_1}{2}z + \left(-\frac{a_1^2}{8} + \frac{a_2}{2}\right)z^2 + \left(\frac{a_1^3}{16} - \frac{a_1 a_2}{4} + \frac{a_3}{2}\right)z^3$$
$$+ \left(-\frac{5a_1^4}{128} + \frac{3a_1^2 a_2}{16} - \frac{a_1 a_3}{4} - \frac{a_2^2}{8} + \frac{a_4}{2}\right)z^4 + O(z^5).$$

Our main equation of interest is the characteristic equation $T_B(s) = \omega'^2$ which we would like to solve for certain values of ω'. In general, solving this characteristic equation amounts to solving an equation $f(s) = w$ where s is complex, $f(s)$ is analytic everywhere except for a finite number of poles, and w is another complex-valued variable. Solving the equation $f(s) = w$ for $g = s(w)$ is reduced then to inverting the function $f(s)$, that is $s = f^{-1}(w)$. In the case when $f(s_0) = w_0$ and $\partial_s f(s_0) \neq 0$, the inverse function $f^{-1}(w)$ is well-defined and analytic in a vicinity of w_0 and its Taylor series can be effectively found using Theorem A.2.1

In the case when $\partial_s f(s_0) = 0$, we refer to s_0 as a *critical point.* More precisely, we refer to s_0 as a *critical point of order* $n \geq 2$ if

$$\partial_s f(s_0) = \cdots = \partial_s{}^{n-1}(s_0) = 0, \quad \partial_s{}^n f(s_0) \neq 0. \tag{20}$$

In the case of a critical point the inverse function $f^{-1}(w)$ becomes multiple-valued in a

vicinity of s_0 and is represented by a convergent *Puiseux series*, that is a series involving fractional powers of the relevant variable [27].

The multiple solutions to the equation $f(s) = w$ in a vicinity of a critical point s_0 satisfy the following statement [16],[17], [27].

Theorem A.2.3 (inverse function at a critical point)**.** Let $f(s)$ be an analytic function in $|s - s_0| < R$, where s_0 is a critical point of order $n \geq 2$ satisfying eq. (20), and $f(s_0) = w_0$. Then there exists a function $g(z)$ analytic for sufficiently small $|z|$ such that the numbers

$$s(w) = s_0 + g\left(|w - w_0|^{\frac{1}{n}}\zeta^m\right), \quad 0 \leq m \leq n-1, \quad \zeta = \exp\left(\frac{2\pi}{n}i\right), \tag{21}$$

represent all solutions to the equation $f(s) = w$.

A.3 The Implicit Function Theorem

Here we formulate the Implicit Function Theorem given in [12] which is used in chapter 4 to establish that the imaginary part of solutions to eq. (4.29) are bounded.

Theorem A.3.1 (The Implicit Function Theorem)**.** Let $\mathcal{A}, \mathcal{B}$ be Banach spaces and let $\mathcal{X}$ be a metric space with metric d. Let G be a continuous function defined in a neighborhobod of $(x_0, y_0) \in \mathcal{X} \times \mathcal{A}$, with values in $\mathcal{B}$, such that

$$G(x_0, y_0) = 0. \tag{22}$$

Suppose that for each fixed x near x_0, the slice function $y \to G(x, y)$ is differentiable with derivative $G_2(x, y)$ depending continuously on x and y. Suppose, furthermore, that $G_2(x_0, y_0)$ is an invertible operator from $\mathcal{A}$ to $\mathcal{B}$. Then:

1. There exist $r > 0, \rho > 0$ such that for each $x \in B(x_0, r)$, there is a unique $f(x) \in B(y_0, \rho)$ satisfying

$$G(x, f(x)) = 0. \tag{23}$$

2. The function f depends continuously on x.

3. If $\mathcal{X}$ is a Banach space and the slice function $x \to G(x, y_0)$ is differentiable at x_0, with derivative $G_1(x_0, y_0)$. Then f is differentiable at x_0 and

$$f'(x_0) = -G_2(x_0, y_0)^{-1} G_1(x_0, y_0). \tag{24}$$

4. If the partial derivative $G_1(x, y)$ exists and is continuous near (x_0, y_0), then f is continuously differentiable near x_0.

Bibliography

[1] M. Abramowitz and I. A. Stegun. *Handbook of Mathematical Functions with Formulas, Graphs, and Mathematical Tables*. Dover, New York, ninth dover printing, tenth gpo printing edition, 1964. A.2

[2] G. Bekefi and K. D. Jacobs. Two-stream, free-electron lasers. *Journal of Applied Physics*, 53:4113 – 4121, 07 1982. 1.1

[3] D. Bohm and E. P. Gross. Theory of plasma oscillations. a. origin of medium-like behavior. *Phys. Rev.*, 75:1851–1864, Jun 1949. 1.1

[4] D. C. *Physics Of Nonneutral Plasmas*. World Scientific Publishing Company, 2001. 1.1

[5] C. Carathéodory. *Theory of Functions of a Complex Variable*. Number v. 1 in AMS Chelsea Publishing Series. American Mathematical Society, 2001. A.2

[6] F. Chen. *Introduction to Plasma Physics and Controlled Fusion: Volume 1 : Plasma Physics*. Introduction to plasma physics and controlled fusion. Plenum Press, 1984. 1.1

[7] L. J. Chu and J. Jackson. Field theory of traveling-wave tubes. *Proceedings of the IRE*, 36:853–863, 1948. 1.1

[8] J. M. Dawson. Plasma oscillations of a large number of electron beams. *Phys. Rev.*, 118:381–389, Apr 1960. 1.1

[9] A. Figotin. An analytic theory of multi-stream electron beam in traveling wave tube. Forthcoming. 1.4

[10] A. Figotin and G. Reyes. Multi-transmission-line-beam interactive system. *J. Math. Phys.*, 54(11):111901, 35, 2013. 1.1, 1.4, 1.4

[11] J. P. Freund, M. A. Kodis, and N. R. Vanderplaats. Self-consistent field theory of a helix traveling wave tube amplifier. *IEEE Transactions on Plasma Science*, 20(5):543–553, Oct 1992.

[12] T. Gamelin and R. Greene. *Introduction to Topology*. Dover books on mathematics. Dover Publications, 1999. A.3

[13] I. Gelfand, M. Kapranov, and A. Zelevinsky. *Discriminants, Resultants, and Multidimensional Determinants*. Modern Birkhäuser Classics. Birkhäuser Boston, 2008.

[14] A. Gilmour. *Principles of Traveling Wave Tubes*. Artech House radar library. Artech House, 1994. 1.1

[15] A. Gilmour. *Klystrons, Traveling Wave Tubes, Magnetrons, Crossed-field Amplifiers, and Gyrotrons*. Artech House microwave library. Artech House, 2011. 1.2

[16] E. Hille. *Analytic function theory. Vol. 1.* Introduction to Higher Mathematics. Ginn and Company, Boston, 1959. A.2

[17] E. Hille. *Analytic function theory. Vol. II.* Introductions to Higher Mathematics. Ginn and Co., Boston, Mass.-New York-Toronto, Ont., 1962. 4.3.2, A.1, A.2

[18] A. V. Hollenberg. Experimental observation of amplification by interaction between two electron streams. *Bell System Technical Journal*, 28(1):52–58, 1949. 1.1

[19] N. Krall and A. Trivelpiece. *Principles of Plasma Physics [by] Nicholas A. Krall [and] Alvin W. Trivelpiece*. International series in pure and applied physics. McGraw-Hill, 1973. 1.1

[20] B. N. *Electromagnetic Theory And Applications In Beam-wave Electronics*. World Scientific Publishing Company, 1996. 1.1

[21] P. M. Phillips, E. G. Zaidman, H. P. Freund, A. K. Ganguly, and N. R. Vanderplaats. Review of two-stream amplifier performance. *IEEE Transactions on Electron Devices*, 37(3):870–877, March 1990. 1.1

[22] J. R. Pierce. Traveling-wave tubes. *Bell System Technical Journal*, 29(3):390–460, 1950. 1.1, 1.3

[23] J. R. Pierce. Waves in electron streams and circuits. *Bell System Technical Journal*, 30(3):626–651, 1951. 1.1, 1.3

[24] J. R. Pierce and W. B. Hebenstreit. A new type of high-frequency amplifier. 1949. 1.1

[25] S. Ramo. Currents induced by electron motion. *Proceedings of the IRE*, 27:584–585, 1939. 1.1

[26] L. Schächter. *Beam-Wave Interaction in Periodic and Quasi-Periodic Structures*. 01 2011. 1.1

[27] B. Simon. *Advanced Complex Analysis: A Comprehensive Course in Analysis, Part 2B*. Number v. 2, pt. 2 in A comprehensive course in analysis. American Mathematical Society, 2015. 4.5, A.2

[28] T. Stix. *Waves in Plasmas*. American Inst. of Physics, 1992. 1.1

[29] S. Tsimring. *Electron Beams and Microwave Vacuum Electronics*. Wiley Series in Microwave and Optical Engineering. Wiley, 2006. 1.1